AD NUMBER

AD489154

LIMITATION CHANGES

TO:

Approved for public release; distribution is unlimited.

FROM:

Distribution authorized to U.S. Gov't. agencies and their contractors; Critical Technology; NOV 1965. Other requests shall be referred to Air Force Materials Laboratory, Attn: MAMC, Wright-Patterson AFB, OH 45433. This document contains export-controlled technical data.

AUTHORITY

WPAF/IST ltr, 21 Mar 1989

AFML-TR-65-2
Part II, Volume VI

TERNARY PHASE EQUILIBRIA IN TRANSITION METAL-BORON-CARBON-SILICON SYSTEMS

Part II. Ternary Systems
Volume VI. Zr-Hf-B System

D. P. Harmon
Aerojet-General Corporation

TECHNICAL REPORT NO. AFML-TR-65-2, Part II, Volume VI

November, 1965

Air Force Materials Laboratory
Research and Technology Division
Air Force Systems Command
Wright-Patterson Air Force Base, Ohio

AFML-TR-65-2
Part II, Volume VI

TERNARY PHASE EQUILIBRIA IN TRANSITION METAL-BORON-CARBON-SILICON SYSTEMS

Part II. Ternary Systems
Volume VI. Zr-Hf-B Systems

D.P. Harmon

BLANK PAGE

FOREWORD

The work described in this report has been carried out at the Materials Research Laboratory, Aerojet-General Corporation, Sacramento, California under USAF Contract No. AF 33(615)-1249. The contract was initiated under Project No. 7350, Task No. 735001, and was administered under the direction of the Air Force Materials Laboratory, Research and Technology Division, with Captain R. A. Peterson and Lt. P.J. Marchiando acting as Project Engineers, and Dr. E. Rudy, Aerojet-General Corporation as Principal Investigator. Professor Dr. Hans Nowotny, University of Vienna served as consultant to the project.

The project, which includes the experimental and theoretical investigation of selected ternary systems in the system classes Me_1-Me_2-C, Me-B-C, Me_1-Me_2-B, Me-Si-B, and Me-Si-C, was initiated on 1 January 1964.

The author wishes to acknowledge the guidance given by Dr. E. Rudy during the course of the investigation, and to thank Dr. Y.A. Chang for his consultation on the thermochemical evaluation of the system. The support given by J. Hoffman, R. Cobb, and E. Spencer in the experimental work is also gratefully appreciated. The report was technically proofread by Dr.A.J. Stosick, and the author is indebted to him for his many helpful criticisms.

The chemical analytical work was carried out under the supervision of Mr. W.E. Trahan, Quality Control Division. The drawings were prepared by R. Cristoni and Mrs. J. Weidner typed the report.

The manuscript of this report was released by the author in November, 1965 for publication as an RTD Technical Report.

Other reports issued under USAF Contract AF 33(615)-1249 have included:

Part I. Related Binaries
- Volume I. Mo-C Systems
- Volume II. Ti-C and Zr-C Systems
- Volume III. Mo-B and W-B Systems
- Volume IV. Hf-C System
- Volume V. Ta-C System. Partial Investigation of the Systems V-C and Nb-C
- Volume VI. W-C System, Supplemental Information on the Mo-C System
- Volume VII. Ti-B System
- Volume VIII. Zr-B System
- Volume IX. Hf-B System

Part II. Ternary Systems
Volume I. Ta-Hf-C System
Volume II. Ti-Ta-C System
Volume III. Zr-Ta-C System
Volume IV. Ti-Zr-C, Ti-Hf-C and Zr-Hf-C System.
Volume V. Ti-Hf-B System

Part III. Special Experimental Techniques
Volume I. High Temperature Differential Thermal Analysis

Part IV. Thermochemical Calculations
Volume I. Thermodynamic Properties of Group IV, V, and VI Binary Transition Metal Carbides.

This technical report has been reviewed and is approved.

W. G. RAMKE
Chief, Ceramics and Graphite Branch
Metals and Ceramics Division
Air Force Materials Laboratory

ABSTRACT

The ternary system zirconium-hafnium-boron has been established for temperatures above 750°C with the aid of melting point, X-ray, and metallographic investigations of chemically analyzed alloys.

A brief thermochemical evaluation of the system was made at 1400°C, and the Gibbs free energies of formation for both the hafnium monoboride and hypothetical "zirconium monoboride" were calculated.

The zirconium-hafnium system was reviewed using differential-thermal analytical techniques, and the proposed binary diagram is given.

BLANK PAGE

TABLE OF CONTENTS

TABLE OF CONTENTS (Continued)

ILLUSTRATIONS

ILLUSTRATIONS (Continued)

ILLUSTRATIONS (Continued)

TABLES

I. INTRODUCTION AND SUMMARY

A. INTRODUCTION

Intense interest has been given to the borides of the group IV transition metals in recent years due to the desirable properties of the diboride phases (TiB_2, ZrB_2, and HfB_2), i.e. high melting points, high hardness values, and good oxidation characteristics. Although fairly intensive efforts have been made to develop the borides for high temperature applications, little effort has been devoted to the establishment of the basic phase equilibria in the metal-boron binary systems, let alone higher order systems.

Recently, the Air Force initiated a program in this laboratory for the investigation of the phase equilibria in selected transition metal-boron-carbon-silicon ternary systems, and this report covers but one of a number of related investigations on binary and ternary boron-containing systems. It is hoped that the results of these investigations will do much to alleviate the shortage of phase equilibrium data on boron containing systems, moreover, it is intended that the thermochemical data derived from these investigations are to be used in conjunction with available thermodynamic data for the prediction of the phase behavior of uninvestigated higher order systems.

B. SUMMARY

The ternary zirconium-hafnium-boron system has been established using melting point, X-ray, metallographic and chemical analytic investigations. A cursory investigation of the binary zirconium-hafnium system was performed using differential thermal-analytical techniques.

1. Binary Systems

a. Metal-Boron System

The binary zirconium-boron and hafnium-boron systems have recently been extensively investigated and are described in previous documentary reports[1,2].

b. Zirconium-Hafnium Binary

The phase diagram for the system zirconium-hafnium (Figure 1) was established exclusively with differential thermo-analytical investigations of seven binary alloys. It is well known that both metals undergo an allotropic transformation from the low temperature (α) hexagonal close-packed structure to the high temperature (β) body-centered cubic form. In the binary both the α- and β-phases form a continuous series of solid solutions, which are separated by a narrow two-phase ($\alpha + \beta$) region. The transformation temperature varies nearly linearly from 872°C on the zirconium side to ~1810°C on the hafnium side. Lattice parameter measurements of the α-solid solution (hcp) also show a linear dependence. The extrapolated end points yielded values for zirconium, $a = 3.23_2$ and $c = 5.14_8$ Å; and for hafnium, $a = 3.19_5$ and $c = 5.05_{75}$ Å.

Melting point results confirm previous results by E.T. Hayes and D.K. Deardorff[3].

2. Zirconium-Hafnium-Boron Ternary System

A isometric drawing of the experimentally established ternary system is given in Figure 2.

a. Diboride Solid Solution

The main feature of the system is the high-melting solid solution between the isomorphous binary diboride compounds. The maximum solidus of the solution varied smoothly from 3245°C[1] for

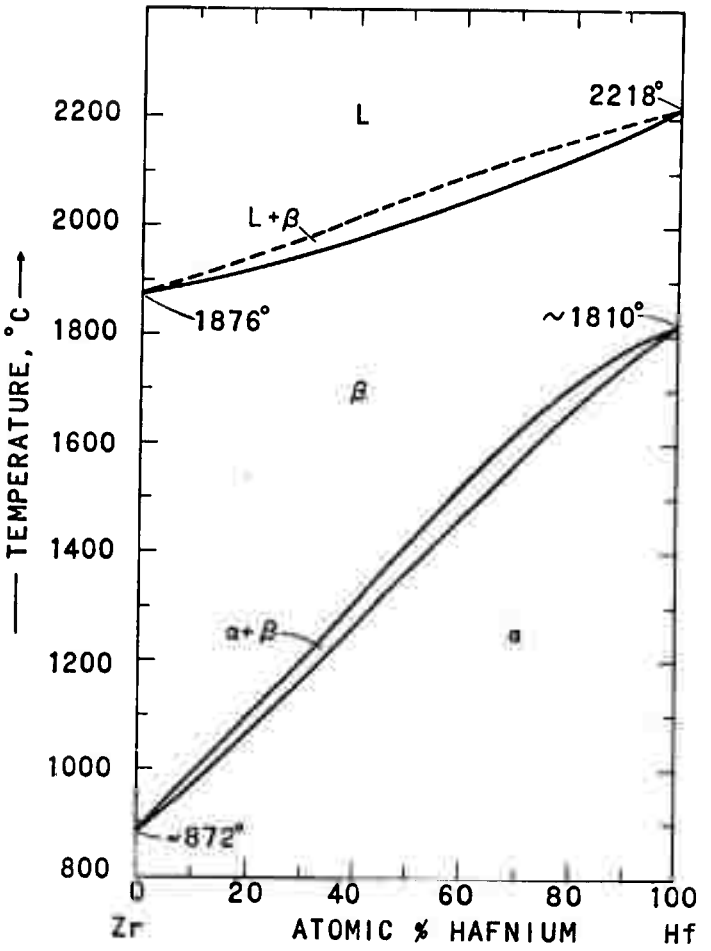

Figure 1. Proposed Zirconium-Hafnium Phase Diagram

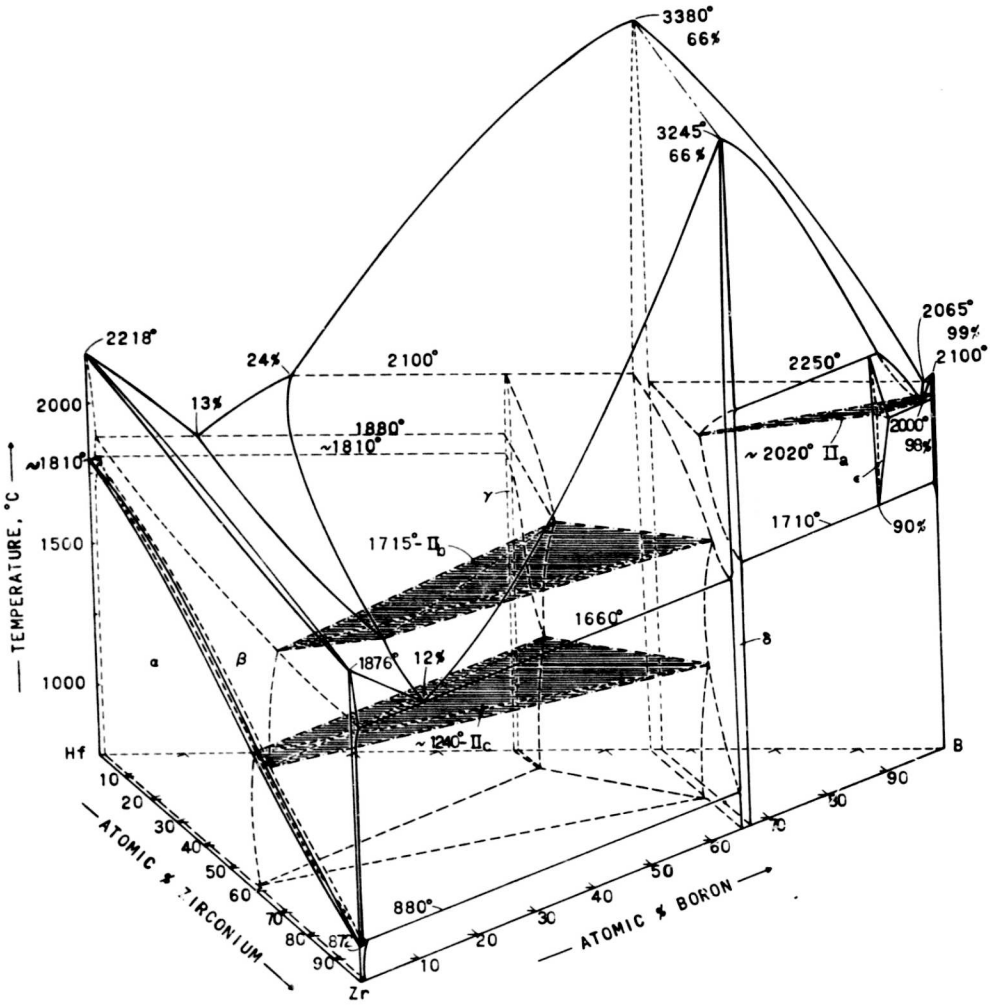

Figure 2. Zirconium-Hafnium-Boron Phase Diagram

ZrB_2 to 3380°C[2] for HfB_2. The lattice constants of the hexagonal solid solution (C-32) varied linearly across the systems, and the extrapolated end parameters were in good agreement with the literature. The following lattice parameters were obtained: ZrB_2, a = 3.16$_8$ and c = 3.53$_3$ Å; HfB_2, a = 3.14$_1$ and c = 3.47$_7$ Å.

A very narrow range of homogeneity was indicated to exist.

b. Metal-Rich Equilibria

In the metal-rich portion of the system two four-phase reaction planes are encountered, both of which are class II* ("two-over-two").

(1) Class II Four-Phase Invariant Plane (1715°C)

At 1715°C an invariant four-phase reaction plane was found to occur. The reaction is of a class II (labled II_b throughout the text) type and can be represented by the following reaction equation:

$$\text{Liquid} + (Hf, Zr)B\ (\gamma) \underset{T \leq 1715°C}{\overset{T \geq 1715°C}{\rightleftharpoons}} \beta\text{-}(Hf, Zr) + (Hf, Zr)B_2(\delta)$$

At this temperature the monoboride phase had its maximum zirconium exchange which was indicated to be ~34 mole % "ZrB".

(2) Class II Four-Phase Invariant Plane (~1240°C)

At this temperature the four phases, $\alpha + \beta + \gamma + \delta$ are in equilibrium with each other. The solid state four-phase reaction (II_c) can be represented as:

---

* Nomenclature used throughout the report is taken from the book "Phase Diagrams in Metallurgy" by F.N. Rhines[4].

$$\beta\text{-(Hf, Zr)} + \text{(Hf, Zr)B}\ (\gamma) \underset{T \leq \sim 1240^\circ C}{\overset{T \geq \sim 1240^\circ C}{\rightleftharpoons}} \alpha\text{-(Hf, Zr)} + \text{(Hf, Zr)B}_2(\delta)$$

c. Boron-Rich Phase Equilibria

Only a cursory investigation was made in this portion of the system. In this region at least one four-phase plane is encountered; this invariant plane was estimated to occur at ~2020°C and can be represented by the following reaction:

$$\text{Liquid} + \text{(Hf, Zr)B}_2\ (\delta) \underset{T \leq \sim 2020^\circ C}{\overset{T \geq \sim 2020^\circ C}{\rightleftharpoons}} \text{(Zr, Hf)B}_{12}(\epsilon) + \text{Boron.}$$

Metallographic evidence indicated the three-phase field ($\delta + \epsilon + B$) to extend quite far into the ternary at high temperatures (~2000°C).

A Scheil-Schultz reaction diagram is shown in Figure 3 in which the invariant and univariant binary and ternary reactions (at constant pressure) are summarized. The phase relationships as a function of temperature in the metal-rich region of the ternary system are given in a isopleth at 30 atomic percent boron (Figure 4).

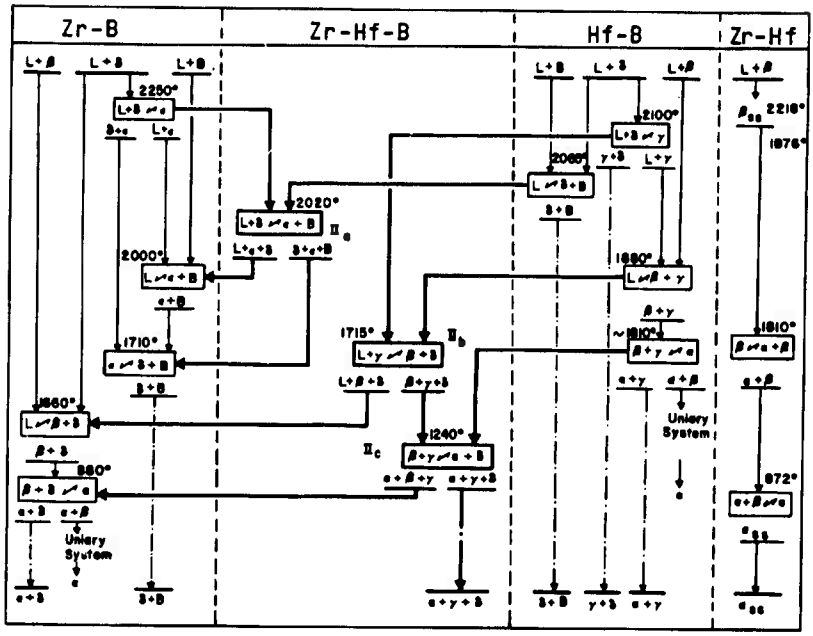

Figure 3. Scheil-Schultz Diagram for the System Zirconium-Hafnium-Boron.

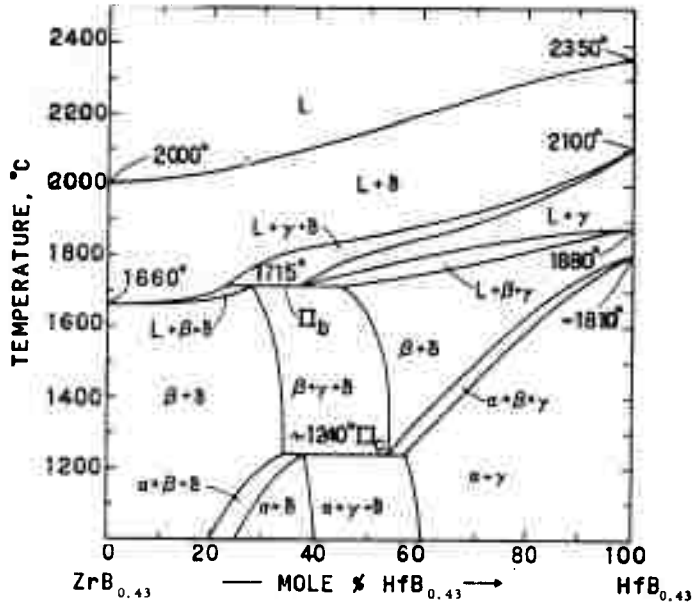

Figure 4. Zr-Hf-B. Isopleth Across 30 Atomic Percent Boron.

II. LITERATURE REVIEW

A. BINARY SYSTEMS

1. Zirconium-Hafnium

The zirconium-hafnium equilibrium diagram as experimentally determined by E. T. Hayes and D. K. Deardorff[3] is shown in Figure 5. J. D. Fast[5] first published a system which was based primarily on theoretical considerations; in this system the α-β transformation curves deviated considerably from ideality (negatively) and the extrapolated value for the α-β transformation in pure hafnium was 1950°C.

Considerable confusion exists in the literature concerning the value for the allotropic transformation temperature of hafnium; Table 1 gives a compilation of many of these values. A possible reason for this confusion is that small impurity elements such as oxygen, carbon, etc. have a drastic effect upon the transformation temperature. The most recent value as determined by E. Rudy[12] is given to be 1795 ± 35°C.

The α-β zirconium transformation has been reported by P. Duwez[13] as being 865°C; investigations in this laboratory are in excellent agreement with this value yielding a temperature of 872°C[14].

C. E. Ells and A. D. McQuillan[15] have indicated that small hafnium additions to zirconium lowers the transformation temperature from 865°C to 800°C, thus indicating that the transformation goes through a minimum. Results by Hayes and Deardorff[3], however, did not indicate such a minimum to exist.

Melting point investigations[3] indicate that the maximum solidus varies smoothly from the melting point of zirconium (1852°C) to the melting point of hafnium (2222°C).

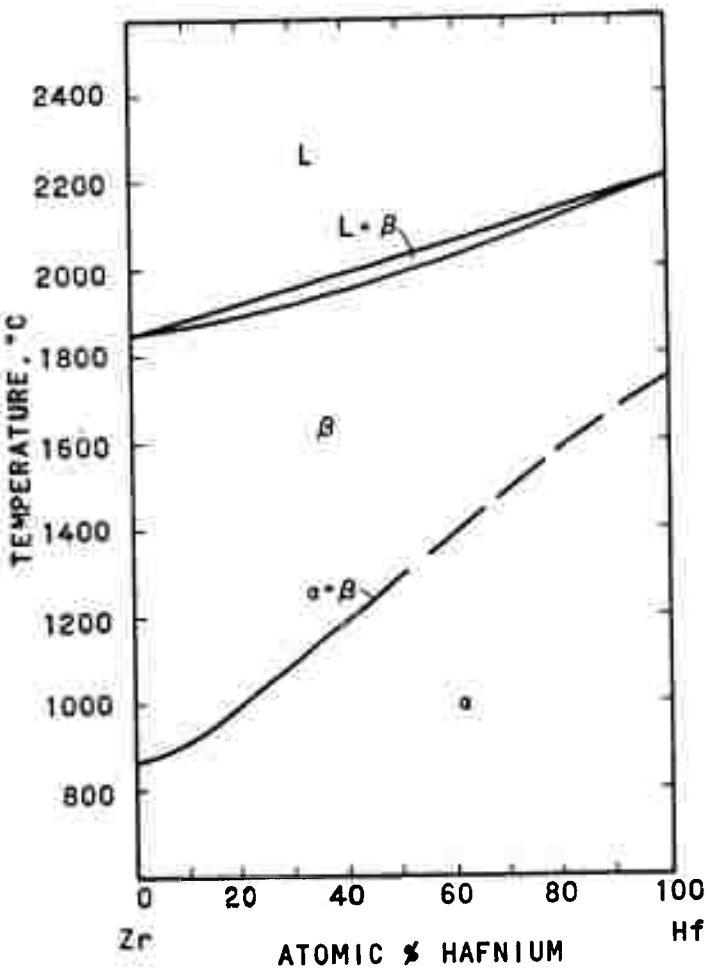

Figure 5. Zr-Hf Phase Diagram
(E.T. Hayes and D.K. Deardorff, 1957).

Table 1. Literature Values for the α-β Hafnium Transformation

Investigator	Ref	α→β Temp. °C	Remarks
Fast, 1952	5	1950°	Extrapolated to 100% Hf
Deardorff and Kato, 1958	6	1760 ± 35°	Extrapolated to 100% Hf
Taylor & Doyle, 1960, 1961	7	1950°	4.41 At% Zr
Grant & Giessen, 1960	8	1840°	4.41 At% Zr
Ross & Hume-Rothery 1963	9	1995 ± 70°	Extrapolated to 100% Hf
R.G. Bedford, 1965	10	1757 ± 30°	Extrapolated to 100% Hf
Romano, Pasche, and Kato, 1965	11	1777°	Extrapolated to 100% Hf
E. Rudy, 1965	12	1795 ± 35°	Extrapolated to 100% Hf

For a thorough review of the system, the works by Hansen[16] should be consulted.

2. Zirconium-Boron

The most recent phase diagram for the zirconium-boron system has been presented by E. Rudy and St. Windisch[1], (Figure 6). The system contains two intermediate compounds, a high melting diboride and a dodecaboride which is stable at intermediate temperatures only. The existence of the "monoboride" previously reported in literature[17, 18, 19]

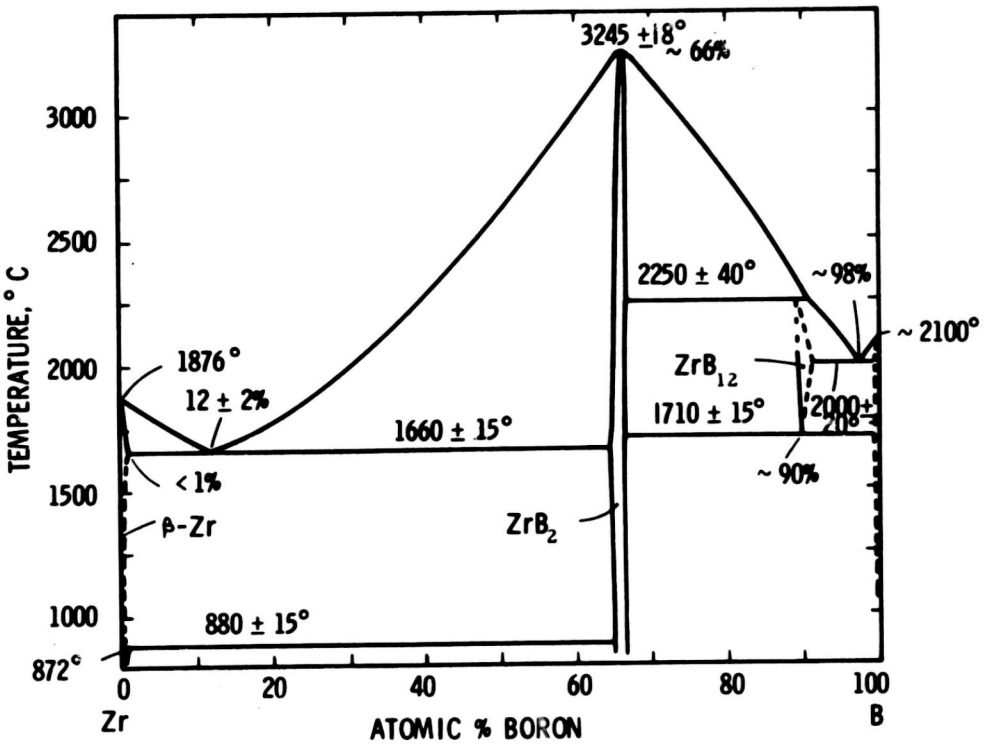

Figure 6. Zirconium-Boron Equilibrium Diagram
(E. Rudy and St. Windisch, 1965).

has not been confirmed by other investigations[20,21,22], and is indicated actually to be impurity oxide, nitride or carbide phase[1,22].

The solid solubility of boron in zirconium has been reported to be nominal (approximately 1 atomic percent)[1,20]. The α-β zirconium transformation temperature is reported to be slightly increased (from 872°C to 880°C) by boron additions, thus indicating a peritectoid decomposition of the α-solid solution into β-zirconium and the diboride phase[1]. Eutectic melting is observed between the metal phase and the diboride; Rudy and Windisch report the eutectic to be at 1660°C and 12 atomic percent boron, whereas Glaser and Post[19], and Schedler[23] place the metal-rich eutectic at 22 atomic percent boron and 1760°C.

The diboride phase crystallizes in a hexagonal type structure (C32)[20]; and the lattice parameters are given as a = 3.167 Å; c = 3.530 Å [1], which are in good agreement with other literature values[20, 22]. The diboride is found to have a rather narrow range of homogeneity(<2 atomic percent boron) and melts congruently at 3245°C[1]. Other values presented by C. Agte (3190 ± 50)[24] and K. Moers (3040°C)[25] are low apparently due to the fact that the maximum melting is extremely difficult to ascertain because of the narrow homogeneity range of the phase. Rudy and Windisch[1] based their melting temperature on results of approximately fifteen alloys around the diboride phase.

The dodecaboride (ZrB_{12}) has a face-centered cubic lattice ($D2_f$) with a lattice parameter of, a = 7.408 Å[1,17,18,22]; the phase was determined to form in a peritectic reaction from liquid and the diboride at 2250°C and decomposes eutectoidally at 1710°C into diboride and boron[1]. Glaser and Post[17], however, indicated the ZrB_{12} phase to melt congruently at 2680°C. A eutectic between ZrB_{12} phase and boron is located at approximately 2000°C and 98 atomic percent boron[1].

3. Hafnium-Boron

The only complete investigation of the hafnium-boron binary system has recently been performed by Rudy and Windisch[2]; Figure 7 gives their experimentally established phase diagram.

The systems contain two intermediate phases, a mono- and a diboride. The monoboride forms a eutectic with β-hafnium at 1880°C and at 13 atomic percent boron[2]. At the eutectic temperature the boron solubility in β-hafnium is indicated to be less than 2 atomic percent. Small boron additions are believed to raise the α-β transformation temperature resulting in a peritectoid type decomposition of the α-hafnium phase into β-hafnium and monoboride. The peritectoid isotherm is reported to be approximately 1800°C[2].

The monoboride phase crystallizes in an orthorhombic (B27) structure with lattice parameters of a = 6.517; b = 3.218, c = 4.919 Å[22].

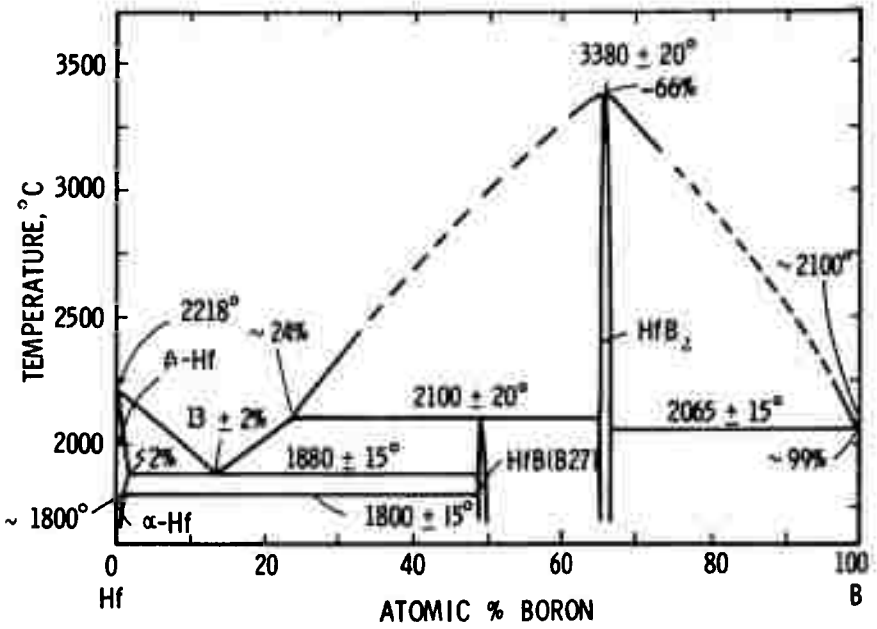

Figure 7. Hafnium-Boron Equilibrium Diagram
(E. Rudy and St. Windisch, 1965)

The previously reported monoboride with a face-centered cubic (B1) structure[26] is probably a result of the presence of an impurity phase, $Hf(O,N,C)_{1-x}$[2,22]. The HfB phase has a limited range of homogeneity (< 1 atomic percent boron)[2]. The phase is reported to form in a peritectic reaction from liquid and diboride at approximately 2100°C[2]. L. Kaufman and E.V. Clougherty[27] indicate the peritectic decomposition temperature for the monoboride to be above 2400°C. Some evidence was given which indicates that the monoboride

is unstable below ~ 1250°C, however, due to the extremely slow reaction rates involved, this could not be conclusively proven[2].

The diboride phase (hexagonal-C32) melts congruently at 3380°C and at approximately 66 atomic percent boron[2]; other melting temperatures by K. Moers[25], F. W. Glaser[26], and R. Kieffer[28] are somewhat lower, but this could be due to extremely narrow range of homogeneity of the HfB_2 phase (<2 At% B). The value quoted by Rudy and Windisch[2] was based on sixteen measurements in the diboride concentration range.

The eutectic between the diboride and boron is located at approximately 99 atomic percent boron and at 2065°C.

B. ZIRCONIUM-HAFNIUM-BORON TERNARY SYSTEM

Very little work is to be found in the literature on the ternary boride alloy systems. Most of the data pertains to the diboride pseudo-binary systems; for the zirconium-hafnium-boron system only one lattice parameter measurement by B. Post, et.al.[29], of a $(Zr,Hf)B_2$ alloy (Zr:Hf = 1:1) has been given a = 3.155; c = 3.497 Å. These authors[29] also indicate that the diborides form a continuous series of solid solutions. Work by K.C. Antony and W.V. Cummings[30] showed, that when zirconium metal powder was mixed with hafnium diboride and heated to 1000°C, HfB_2, ZrB(?), and ZrB_2 were observed in X-ray diffraction patterns. No further work on the ternary alloy system could be located in the literature.

For a detailed evaluation of the literature on the boride system, zirconium-boron, hafnium-boron, as well as zirconium-hafnium-boron, the book by R. Kieffer and F. Benesovsky[31] should be consulted.

III. EXPERIMENTAL PROGRAM

A. STARTING MATERIALS

1. Zirconium-Hafnium Binary Alloys

Elemental zirconium and hafnium sponge were used as starting materials for the binary alloys. The zirconium sponge was purchased from Wah Chang Corp., Albany, Oregon, and had the following major impurities (in ppm): Al-142, Cl-<181, Cr-72, Fe-1331; Mg-<198, N-21, O-862, Si-<55, the hafnium content was 0.6 atomic percent.

The hafnium sponge also purchased from the Wah Chang Corp., had the analyzed impurity levels of (in ppm): Al-94, Cu-<40, Fe-185, Cl-100, Mg-450, N-30, O-680, Ti-250; the zirconium content was 4 atomic percent.

2. Zirconium-Hafnium-Boron Ternary Alloys

The starting materials used for the present investigations were elementals, hydrides, as well as pre-prepared diboride powders. The zirconium metal powder (Wah Chang Corp.) had a particle size of <74 μ, and the impurities were given as (in ppm): C-40, Nb-<100, Cu-61, Fe-315, H-270, Hf-67, N-34, O-830, Ta-<200, Ti-<20, W-<25. The lattice parameter for the material was calculated to be, a = 3.232, c = 5.149 Å, which is in good agreement with the literature value of a = 3.231, c = 5.148 Å[32].

The zirconium dihydride (Wah Chang Corp.) had a hydrogen content of 2.1 weight percent and a particle size of <44μ. The main impurity constituents were reported as (in ppm): C-320, Nb-<100, Cu-125, Fe-1800, Hf-137, Mg-225, N-116, O-1300, Si-157, Ta-<200, Ti-29, and W-<25. An overexposed X-ray diffraction pattern showed only the tetragonal $ZrH_{\sim 2}$ pattern.

The hafnium metal powder (Wah Chang Corp.) had a particle size of <74 μ, and analyzed impurities of (in ppm): C-30, Nb-<100, Fe-70, H-35, N-57, O-550, Si-<50, Ta-<200, Ti-55, W-<20. The zirconium content was 2.77 weight percent.

The boron powder had a purity level of 99.55% with the main impurities being, Fe-0.25%, and carbon 0.1%; the supplier was United Mineral and Chemical Corp., New York.

The diborides (ZrB_2 and HfB_2) were prepared from elemental metal and boron powders. The master alloys were prepared in a previously described[1,2] two step process to circumvent the violent reaction arising from the diboride formation. The final products are powders of <60 μ; the HfB_2 had a boron content of 11.19 weight percent (67.6 atomic percent) and the ZrB_2 had a boron content of 17.14 weight percent (63.5 atomic percent). Spectrographic analysis of the powders gave results similar to the starting metal powders; the carbon content of the HfB_2 alloy powder was approximately 110 ppm, whereas for the ZrB_2 material, 0.16 weight percent.

B. EXPERIMENTAL PROCEDURES

1. Alloy Preparation and Heat Treatment

a. Zirconium-Hafnium Binary Alloys

Seven alloys were prepared in the binary system. The samples were prepared for differential thermal-analytical investigations by arc-melting zirconium and hafnium sponge materials. Each button was melted and then turned over and remelted; the samples were melted four times using this procedure. Prior to running in the DTA the alloys were homogenized at 1200°C in high vacuum ($< 10^{-5}$ Torr) for 2 hours;

each button was subsequently drilled to form a black-body cavity for temperature measurements during the DTA runs.

b. Zirconium-Hafnium-Boron Ternary Alloys

All ternary alloys for solid state, as well as melting point investigation were prepared by hot-pressing intimate mixtures of the powder starting material in graphite dies. The solid state alloys were pressed into cylindrical compacts of approximately 14 mm dia. x 7 mm high, whereas the melting point specimens were hot-pressed into long cylindrical compacts approximately 9.5 mm dia. x 30 mm long. All surfaces were ground to remove any graphite contamination prior to heat treating or melting the alloys.

Alloys for the solid state investigations were heat treated for approximately 100 hours at 1400°C in a tungsten mesh furnace under high vacuum ($< 5 \times 10^{-5}$ Torr). The samples were helium quenched at the termination of the heat treatment by rapidly admitting high purity helium into the furnace chamber. Figure 8 gives the compositions of alloys used for the solid state investigation.

Arc-melted alloys were made for portions of the solid state and/or melting point samples, and were arc-melted in a non-consumable tungsten-arc-melting furnace; in certain cases portions of these alloys were subsequently equilibrated at 1400°C for solid state investigation. Figure 9 shows the composition of the alloys which were arc-melted.

All solid state, arc-melted, as well as melting point alloys were prepared for X-ray diffraction analyses subsequent to the respective heat-treatments. The majority of the melting point and arc-melted alloys were examined metallographically; systematic boron analyses were performed on the above alloys.

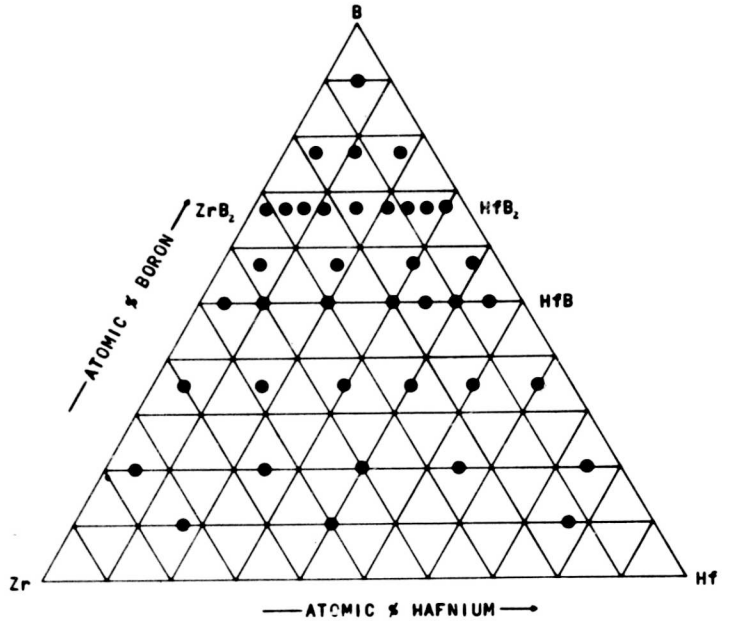

Figure 8. Compositions of Alloys for Solid State Investigation at 1400°C.

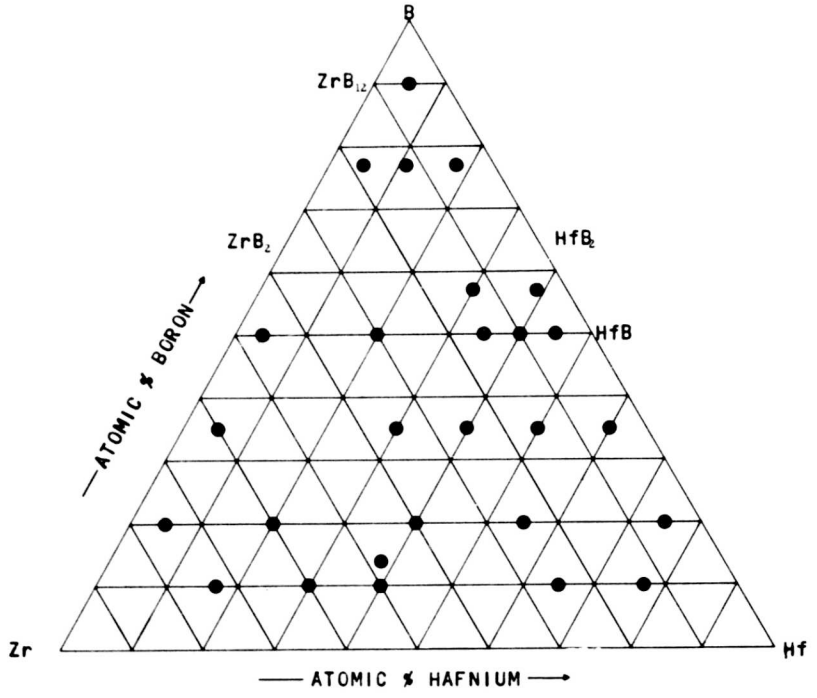

Figure 9. Compositions of Arc-Melted Alloys

2. Differential Thermal Analysis

Differential thermal-analytical investigations were performed on the zirconium-hafnium binary alloys only. The operating principles and procedures for the DTA used in this laboratory have been adequately described elsewhere[33, 34]. Briefly, this apparatus records the temperature differences, if any, between a reference sample which is known to undergo no phase changes (in our experiments, graphite) and that of the test sample as the temperature of both is increased. This is accomplished by focusing the emitted radiation from the black body hole of both samples onto a photo cell and then alternately interrupting the focused beam by a chopping mechanism (Figure 10). If a temperature difference does exist between the two samples, a square wave is produced which ultimately results in a deflection in the ΔT-axis on a plotter which records ΔT versus temperature. The actual temperature of the test sample is monitored separately by a micropyrometer.

To avoid small carbon additions which drastically increase the α-β transformation temperature of hafnium[12], all runs of hafnium-rich alloys never exceeded the transformation temperature by more than 100°C. The samples were also cycled through the transformation range at least five times to obtain consistent results as well as to ensure that no carbon had been picked up, i.e. the α-β transformation temperature remained constant. Subsequent to obtaining the α-β transformation temperatures, the alloys were heated to melting to obtain the melting point. Since carbon is picked up immediately after melting, the binary melting temperatures are based on one measurement only.

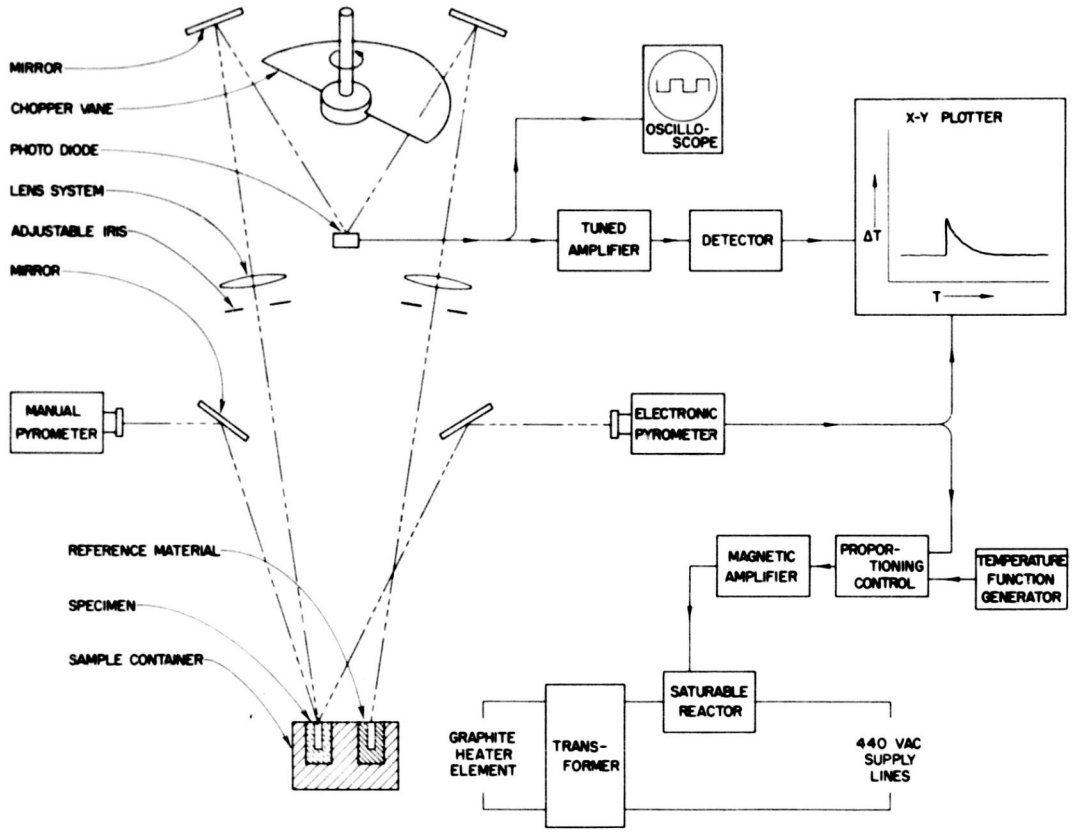

Figure 10. Schematic Drawing of the Experimental Set-up for DTA-Measurements at Elevated Temperatures.

3. Melting Point Investigation

Melting point investigations were performed on approximately fifty ternary alloys (Figure 11). The melting points were determined by the Pirani technique; the furnace and experimental procedures used in these investigations have been described in a previous report under this contract[34]. Figure 12 shows the configuration of the specimen used in these investigations.

Melting point determinations can be carried out in either vacuum or in an inert atmosphere of up to pressures of 2 1/2 atmospheres.

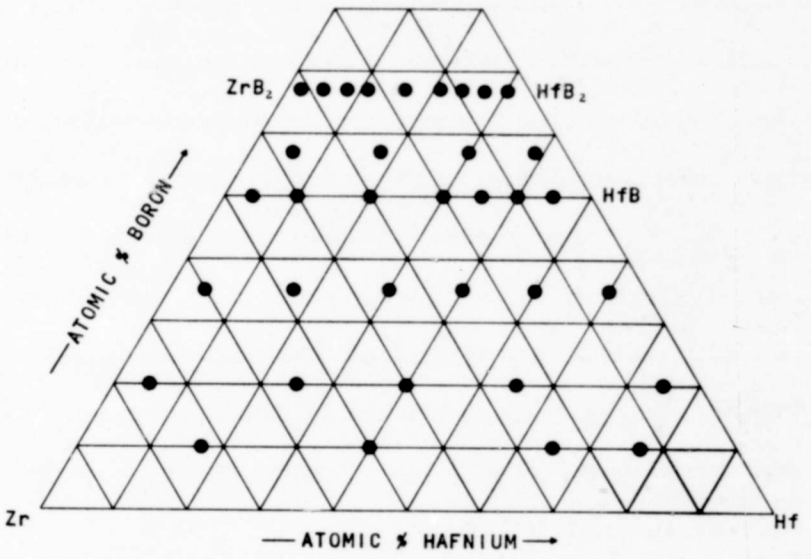

Figure 11. Compositions of Melting Point Alloys in the Zirconium Hafnium-Boron System.

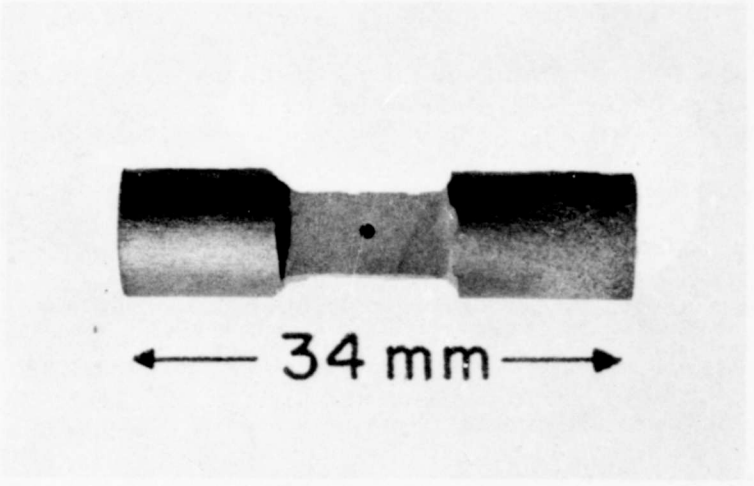

Figure 12. Hot-Pressed, Ground, and Drilled Pirani Melting Point Specimen.

To minimize losses of boron, as well as of metal, the high melting alloys in the diboride regions were melted under 2.3 atmospheres of high purity helium; alloys in the lower melting regions of the system were normally run under 1.3 atmospheres of helium. In all cases the samples were vacuum degassed in the furnace at approximately 1300 to 1500°C prior to melting.

Temperature measurements were carried out with a disappearing-filament type micropyrometer which is calibrated periodically against a certified, standard lamp from the National Bureau of Standards. The temperature corrections for the absorption in the quartz viewing window, as well as for deviations arising from non-black-body conditions have been previously described and validated[34].

4. Metallography

Metallographic investigations were made of melting point, arc-melted, as well as of DTA alloys. Specimens were prepared for metallographic examination by mounting the specimens in a non-conductive diallyl-phthalate base with a conductive lucite-coated copper top which provides an electrical path to the polished sample surface. Samples were rough ground on silicon carbide papers with grit size varying between 120 to 600. Polishing was accomplished on a nylon cloth using a slurry of 0.05 micrometer alumina and Murakami's (or chromic acid) solution.

Alloys which had boron concentrations between 0 and 65 atomic percent were electroetched using either a 10% oxalic acid solution or a 5% sodium hydroxide solution; both solutions yielded excellent results. Single-phase diboride alloys were dip etched in a 10% aqua-regia-hydrofluoric acid solution; specimens in the higher boron concentration region could be examined satisfactorily in the as-polished condition.

5. X-Ray Analysis

Debye-Scherrer powder diffraction patterns using Cr.Kα radiation were made of all samples subsequent to their respective heat treatments.

The crystal structures of all binary phases are known, and identifying and indexing the powder patterns was accomplished with little difficulty. In the metal containing alloys, the low temperature α(Zr,Hf) form was always observed because of the rapid martensitic α-β transformation.

Binary zirconium-hafnium powders were stress-relieved at 800°C for one hour in high vacuum prior to making the X-ray exposures.

6. Chemical Analysis

The wet-chemical method of analysis was used for determining the boron contents of the submitted alloys; the detailed procedures have been described in an earlier documentary report[35]. All melting point alloys in the diboride solid solution region, as well as other selected ternary alloys were analyzed for their total boron contents.

C. RESULTS

1. Zirconium-Hafnium Binary System

Differential thermal-analytical investigations carried out on seven binary alloys showed that hafnium additions raise the α-β transformation temperature from 872°C[14] (Figure 13) for pure zirconium* to 1810 ± 25°C for hafnium. The value for pure hafnium was obtained by extrapolating the α-β curves to the hafnium boundary. A fairly narrow two-phase α-β field was indicated to exist by the differences in the thermal arrest temperatures on the heating and cooling cycles; Figures 14 through 16 show the DTA

*The zirconium sample was prepared from crystal bar stock which was obtained from the Wah Chang Corp., Albany, Oregon.

curves obtained in this investigation. It should be noted (Figures 1 and 17) that with hafnium rich alloys the α-β transformation curves departed slightly from linearity, thus indicating that with low zirconium containing alloys (< 10 atomic percent zirconium) a linear extrapolation cannot be used with complete confidence.

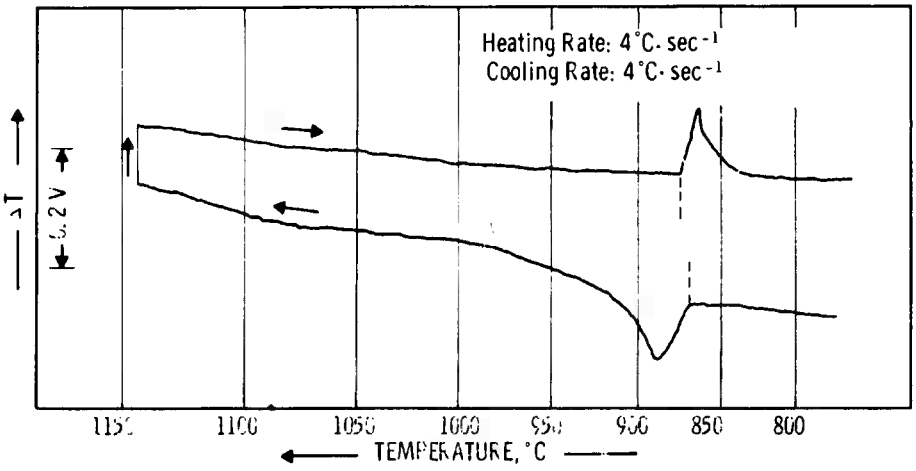

Figure 13. Differential Heating and Cooling Curve for Pure Zirconium.

Previous results in this laboratory have found the α-β hafnium transformation temperature to be at 1795 ± 35°C (extrapolated to pure hafnium) which is in good agreement with the value proposed here. Results given by Hayes and Deardorff[3] (Figure 5 and 17) show a somewhat lower trend for the α-β transformation; however, their melting point data are in excellent agreement with those obtained in the present work. A minimum in the transformation temperatures, which was indicated to exist by Ells and McQuillan[15], was not observed.

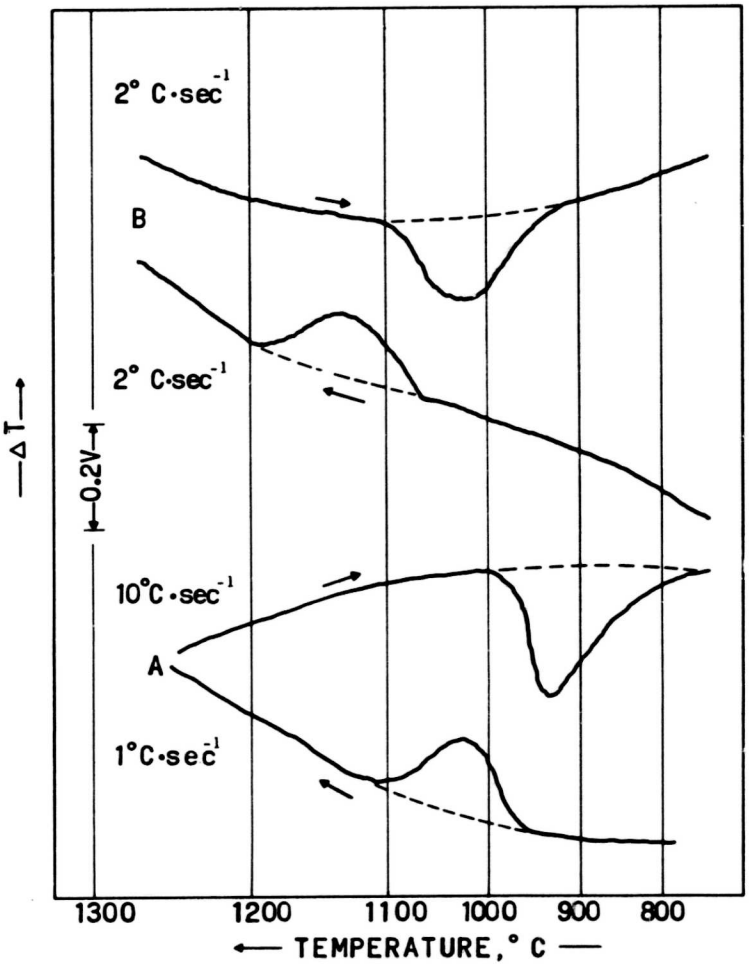

Figure 14. Differential Heating and Cooling Curves of Zirconium-Hafnium Alloys, (A) 10 Atomic Percent Alloy, (B) 20 Atomic Percent Hafnium Alloy.

Lattice parameter values for the low-temperature α-solid solution are given in Figure 18; a linear relationship is evidenced to exist for both a and c parameters. The end point extrapolated values are: zirconium $a = 3.23_{22}$, $c = 5.14_{85}$ Å; hafnium $a = 3.19_{6}$, $c = 5.05_{75}$ Å. These values are in very good agreement with the values given by R.B. Rusell [36];

i.e. for zirconium a = 3.2312, c = 5.1477 Å and for hafnium, a = 3.1946, c = 5.0510.

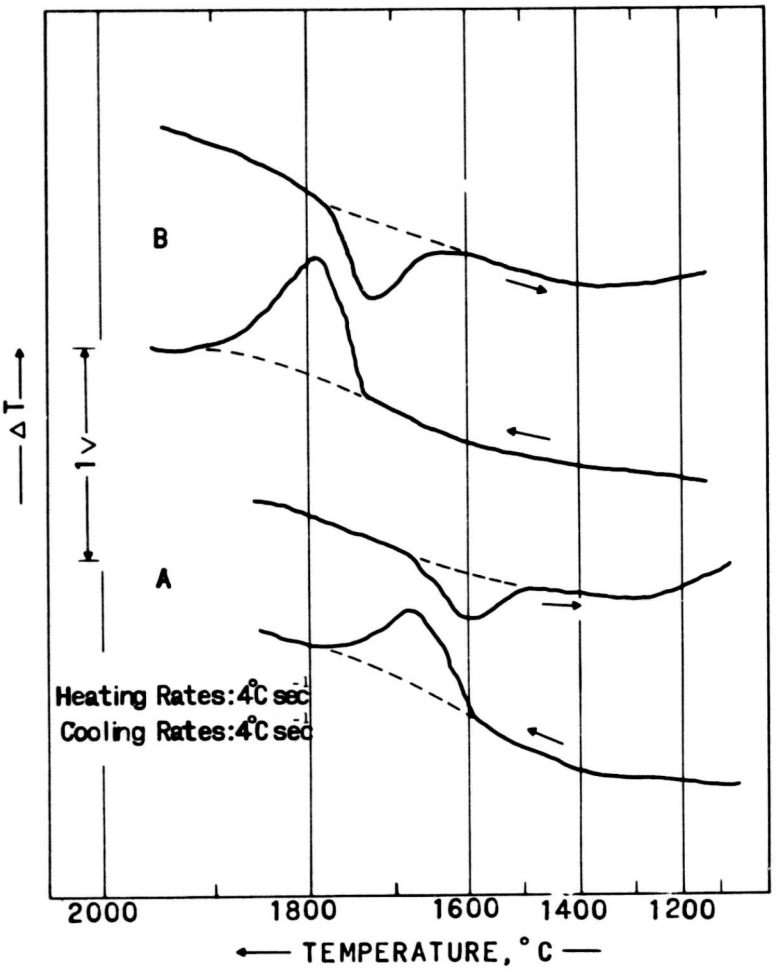

Figure 15. Differential Heating and Cooling Curves of Zirconium-Hafnium Alloys, (A) 75 Atomic Percent Hafnium Alloy, (B) 90 Atomic Percent Hafnium Alloy.

Metallographic analysis of the alloys always showed the α-β transformation structures; typical microstructures obtained from melted alloys are shown in Figures 19 and 20.

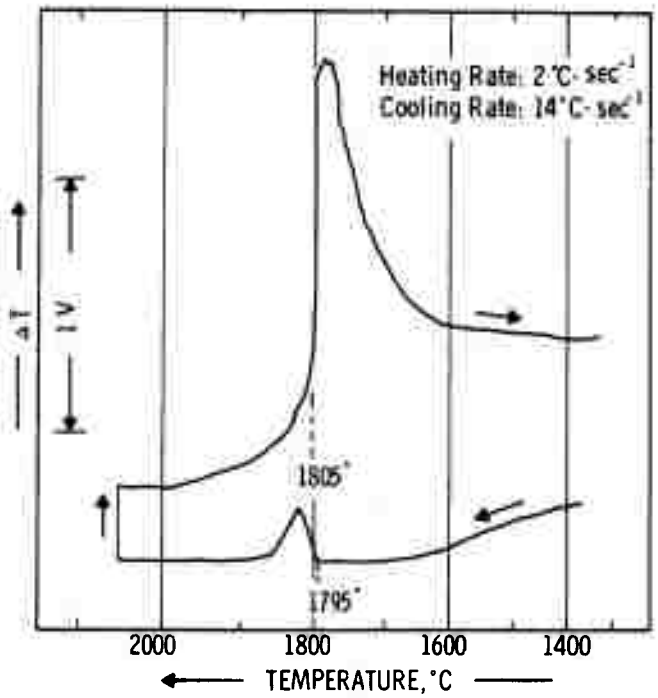

Figure 16. Differential Heating and Cooling Curve of a 4 Atomic Percent Zirconium Alloy in the Zirconium-Hafnium System.

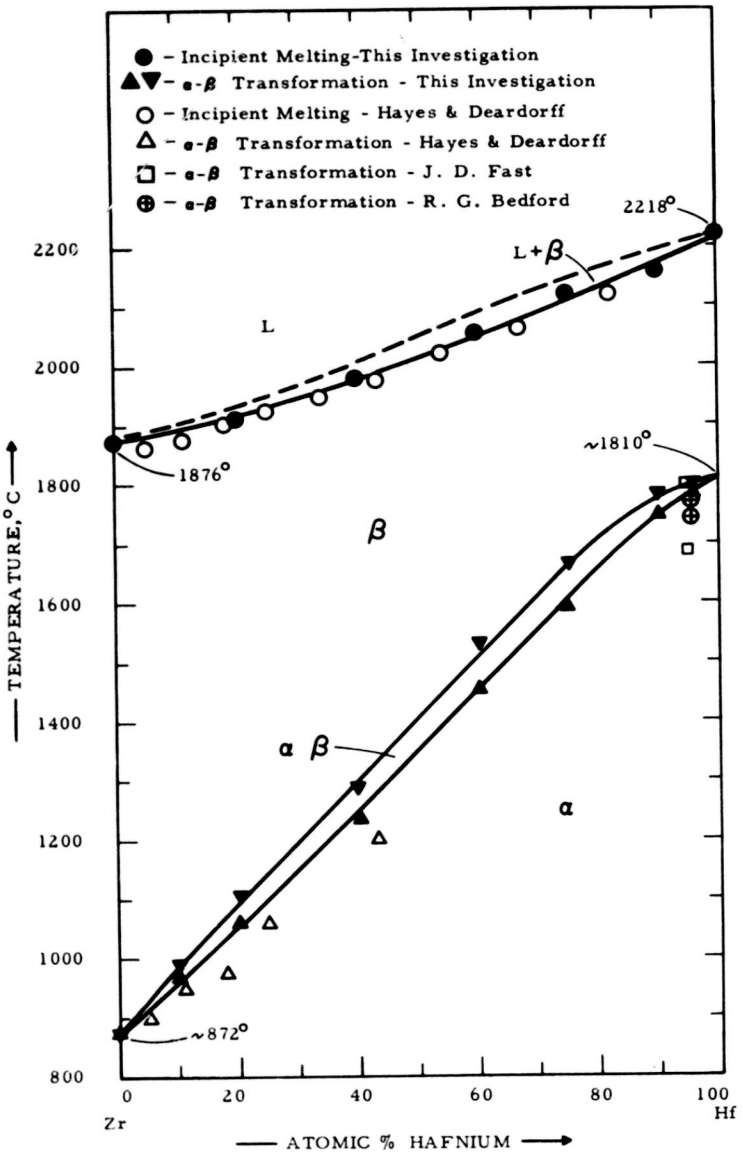

Figure 17. Experimental Data in the Zirconium-Hafnium Binary System.

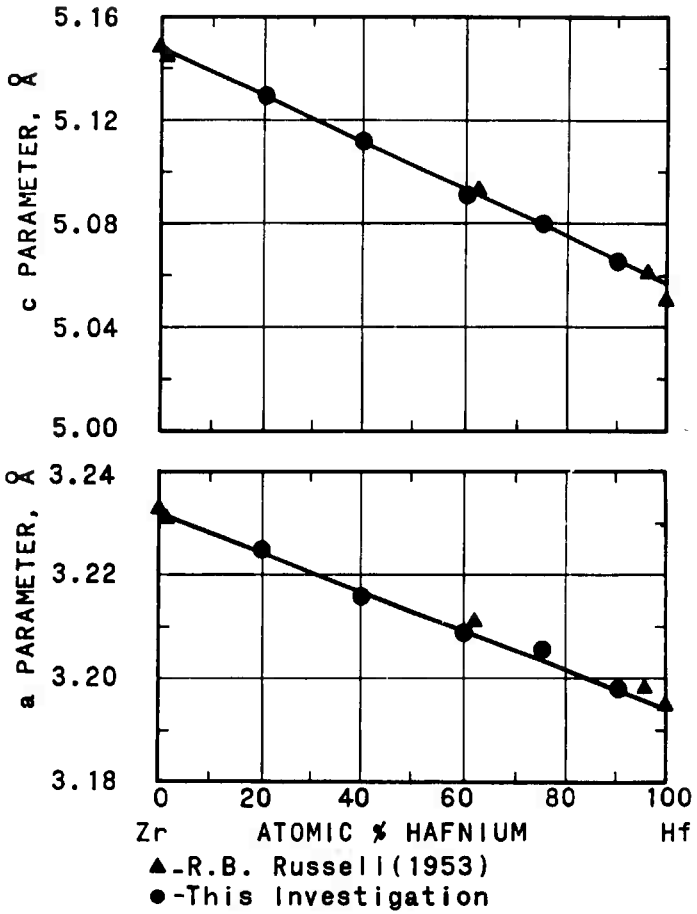

Figure 18. Lattice Parameters of the Hexagonal α-Solid Solution for the Zirconium-Hafnium Alloys.

Figure 19. Zr-Hf (80/20): Arc-Melted, α-β Transformed Structure. X100

Figure 20. Zr-Hf (50/50): Arc-Melted, α-β Transformed Structure. X250

2. Zirconium-Hafnium-Boron Ternary System

A total of forty-one alloy compositions were prepared for solid state investigations in the ternary zirconium-hafnium-boron system. The principal solid-state section was established at 1400°C; phase equilibria reactions at lower and higher temperatures were established with the aid of the boundary systems, indicated tie-line dependencies, melting point data, and metallographic observation. The results in this investigation pertain primarily to the high temperature (> 750°C) phase relationships.

a. Phase Equilibria Below 1400°C

Above approximately 750°C, two three-phase regions ($\alpha + \beta + \delta$ and $\alpha + \gamma + \delta$) are present in the metal-rich portion of the ternary system (Figure 21). The first, ($\alpha + \beta + \delta$), is a result of the α-β two-phase region in the metal-binary system. With increasing temperature this three-phase domain moves across the system towards the hafnium-boron binary, until at approximately 1240°C a four-phase reaction is encountered (Figure 22). At this temperature the isothermal reaction proceeds according to:

$$\beta + \gamma \underset{T \leq \sim 1240}{\overset{T \geq \sim 1240}{\rightleftharpoons}} \alpha + \delta \quad (II_c = \text{Figure 2}),$$

and can be categorized as a Class II reaction. Above 1240°C, the α- and β-phases are in equilibrium with the monoboride phase, and this equilibrium persists toward higher temperatures until approximately 1810°C, whereupon the three-phase region terminates (with increasing temperature, originates with decreasing temperatures) at the binary peritectoid reaction

$$\beta + \gamma \rightleftharpoons \alpha.$$

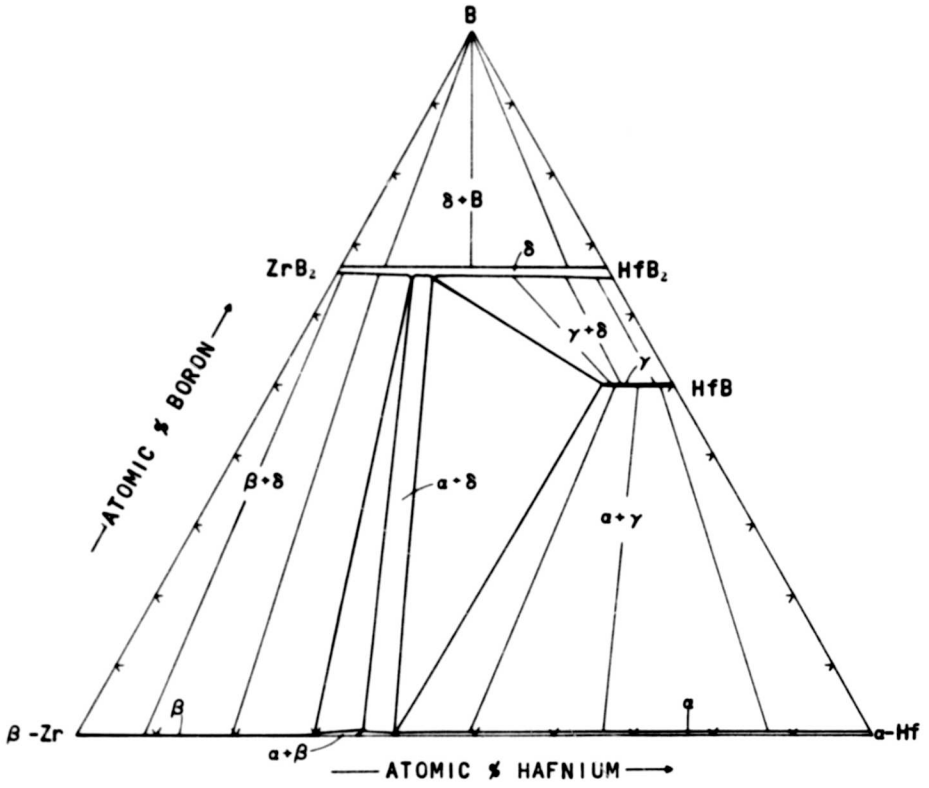

Figure 21. 1200°C Isotherm.

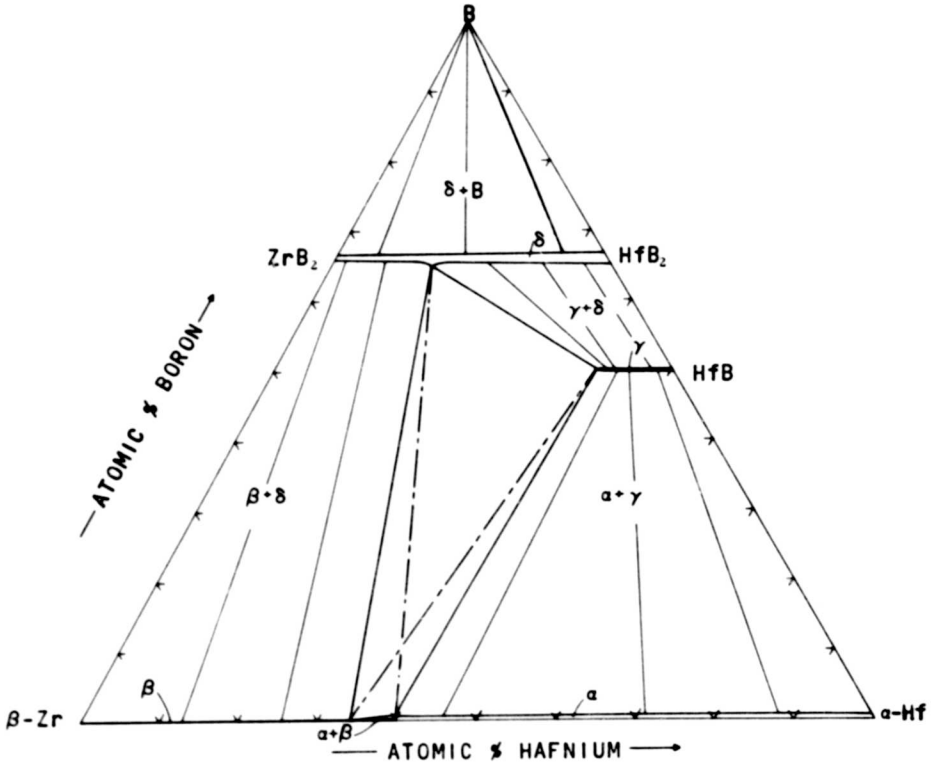

Figure 22. 1240°C Isotherm [Four-Phase Reaction Plane ($\beta + \gamma \leftrightharpoons \alpha + \delta$)].

b. 1400°C Isothermal Section

At this temperature, two three-phase and six two-phase fields exist, along with the single phase diboride, monoboride, α-metal, and β-metal solid solutions (Figure 23).

Lattice parameter measurements of diboride alloys equilibrated at 1400°C show that a complete solid solution exists between the two binary phases (Figure 24); the solution is indicated to follow Vegard's law, since a linear dependence of the ternary parameters is observed. Good agreement with the binary parameters[1,2] is found by extrapolating the ternary values to the boundary systems; the ternary parameters given by B. Post, et.al.[29] also fit the present data well. It should be noted that alloys in the middle of the solid solution region attained equilibrium very slowly, and best results were obtained when the samples were first equilibrated at higher temperatures and then re-equilibrated at 1400°C.

Due to the extreme sluggishness of formation of the hafnium monoboride phase, the exact extent of this solid solution could not be determined from single phase alloys at 50 atomic percent boron, but could only be deduced from X-ray evaluation of two and three-phased (metal, monoboride,and/or diboride) alloys in the lower boron concentration regions. The zirconium exchange was placed at approximately 22 atomic percent; this solid solution is in equilibrium with the zirconium-rich diboride solid solution as well as the high-temperature, body-centered cubic metal solution.

The base point of the three-phase region, $\beta + \gamma + \delta$, along the diboride (δ) solid solution was obtained by comparing the lattice parameters of alloys in the sub-diboride region to the lattice parameters of the diboride solid solution. The base point on the β-metal solid

solution could be determined only from the ternary non-equilibrium metal lattice parameters due to the fact that the β-phase could never be retained upon cooling. These lattice parameter values were compared to those of the metal solid solution which were corrected empirically for boron solubilities by assuming a linear dependency of the parameters from the zirconium-boron binary values[1] to the hafnium-boron binary values[2].

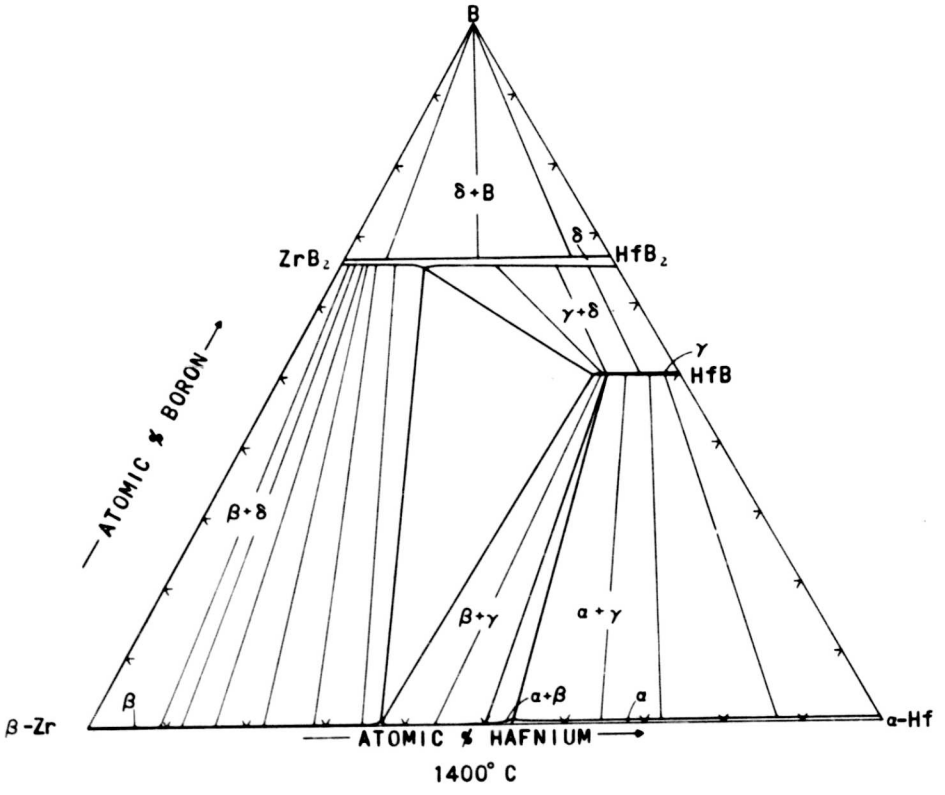

Figure 23. 1400°C Isotherm.

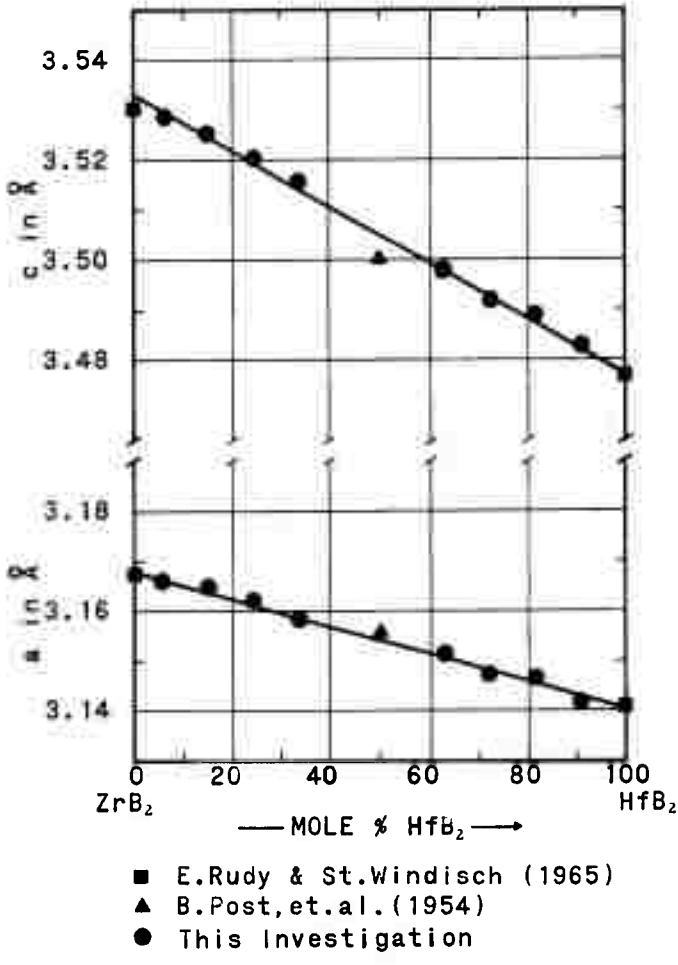

Figure 24. Lattice Parameters of Ternary Diboride Alloys Equilibrated at 1400°C.

c. Higher Temperature Equilibria

For sake of convenient reference, the high-temperature isothermal sections are grouped together at the end of this section. A brief glance should be made of these sections before proceeding further in order to become familiar with the phase equilibria to be discussed (pages 47 to53).

(1) Metal-Rich Equilibria

First melting in the system occurs in the zirconium-boron binary at the metal-rich eutectic temperature of 1660°C. Eutectic trough melting was determined to occur in the metal-rich region of the ternary system with alloys placed at 10 and 20 atomic percent boron. Although the alloys were not placed exactly along the eutectic trough, the location of the trough could be deduced from metallographic analysis of melting point as well as arc-melted alloys. Figures 25-28 show representative metallographic results obtained in these investigations. It should be noted, that in the metal-monoboride two-phase alloys, the monoboride phase tended to agglomerate, even when rapidly quenched during arc-melting. In every instance non-typical eutectic structures were obtained with alloys in this region of the system.

The eutectic trough melting curve can be constructed by establishing the tie-lines in this region and correcting the composition of alloys which are in close proximity to the trough. The incipient melting temperatures of these alloys should correspond to the melting temperatures along the eutectic trough. Figure 29 depicts the composition and melting temperatures of the eutectic trough, as well as the tie-line compositional corrections applied to the alloys.

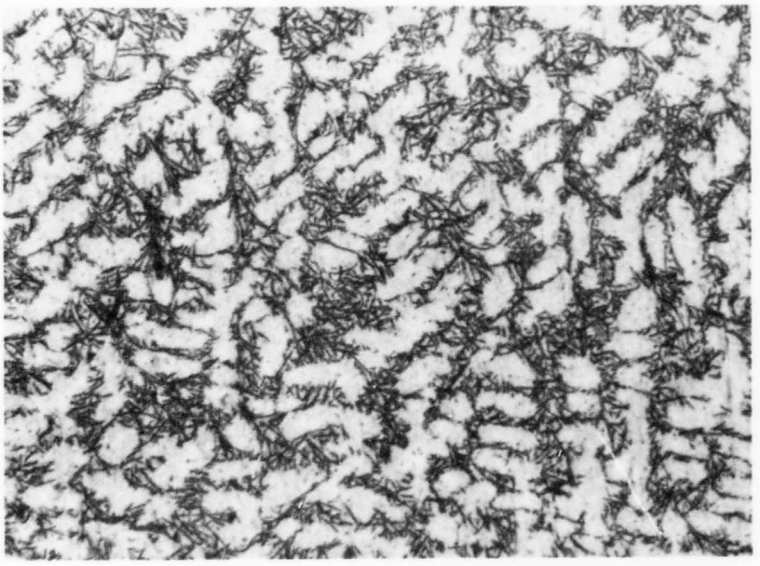

Figure 25. Zr-Hf-B (73/17/10): Arc-Melted Alloy Showing Primary Metal in a Metal-Diboride Eutectic Matrix. X375

Figure 26. Zr-Hf-B (25/65/10): Arc-Melted Alloy Showing Primary Metal in a Metal-Monoboride Eutectic Matrix. X450

Note that Monoboride Grains Tend to Agglomerate, also α-β Transformed Structure is Visible in Metal Grains.

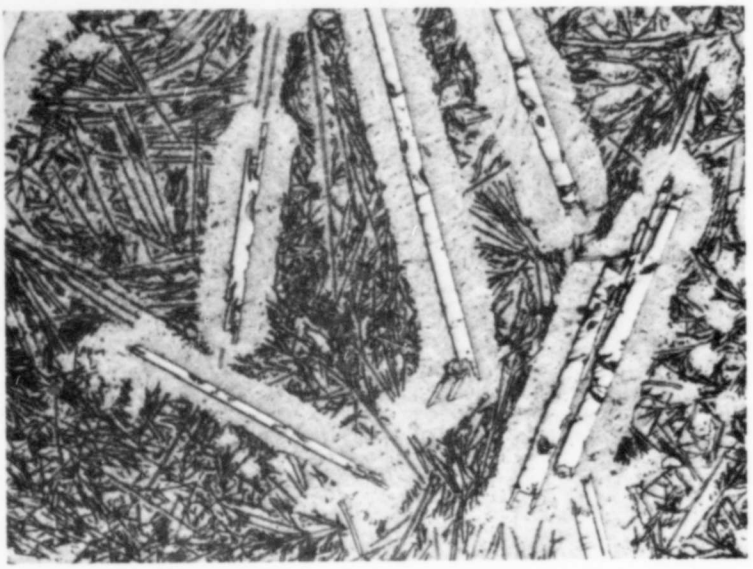

Figure 27. Zr-Hf-B (75/5/20): Arc-Melted Alloy Showing Primary Diboride in a Eutectic Matrix. X375

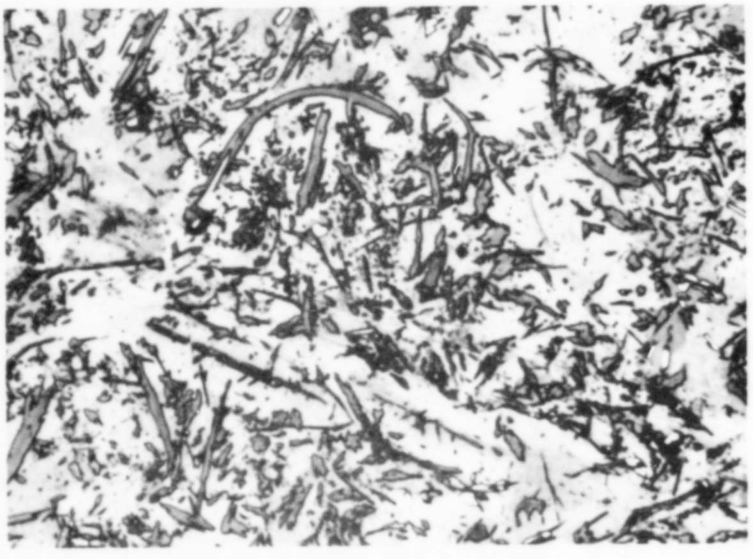

Figure 28. Zr-Hf-B (25/55/20): Arc-Melted Alloy Showing Primary Crystallized Monoboride (Medium-Sized Dark Grey Crystals) in a Metal-Monoboride Eutectic Matrix (Partially Agglomerated). X625

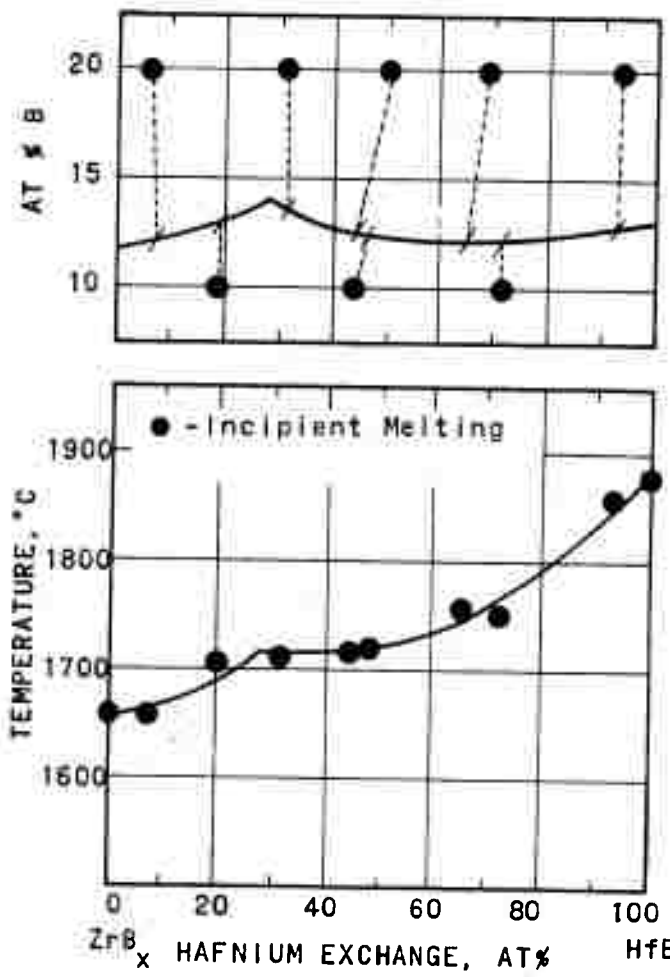

Figure 29. Composition (Top) and Temperature of the Metal-Rich Eutectic Trough in the Zirconium-Hafnium Boron System.

A class II four-phase reaction plane according to

$$L + \gamma \leftrightarrows \beta + \delta \qquad (II_b)$$

is encountered at approximately 1715°C. Examination of the melting point data along the lower boron concentration regions indicated a rather large four-phase field to exist.

At this temperature, the monoboride phase has its greatest zirconium-solubility, which was determined to be approximately 34 mole percent "zirconium monoboride" exchange (Figure 30). However, as previously mentioned, due to the extreme slow formation of the hafnium monoboride solid solution from the metal and diboride phases, equilibrium monoboride alloys were never obtained.

Alloys in the monoboride region which had been melted always showed non-equilibrium two- or three-phased structures (metal-diboride or metal-monoboride-diboride). Long time annealing of these alloys (1400°C) generally resulted in an increased amount of monoboride (compare Figures 31 and 32), but equilibrium structures could not be obtained in reasonable lengths of time with alloys which had boron concentrations near 50 atomic percent.

Best results were obtained from alloys in the two-phase metal-monoboride region of the system; here reactions were found to go to completion at a much faster rate. Figures 33 and 34 show the extent of the monoboride formation upon long time annealing of arc-melted alloys in the lower boron content region. Melting point alloys in this region also yield good results; the collapsing temperatures normally were below the

peritectic temperature, and since the diboride phase never was formed, the above mentioned problems were not encountered (Figure 35).

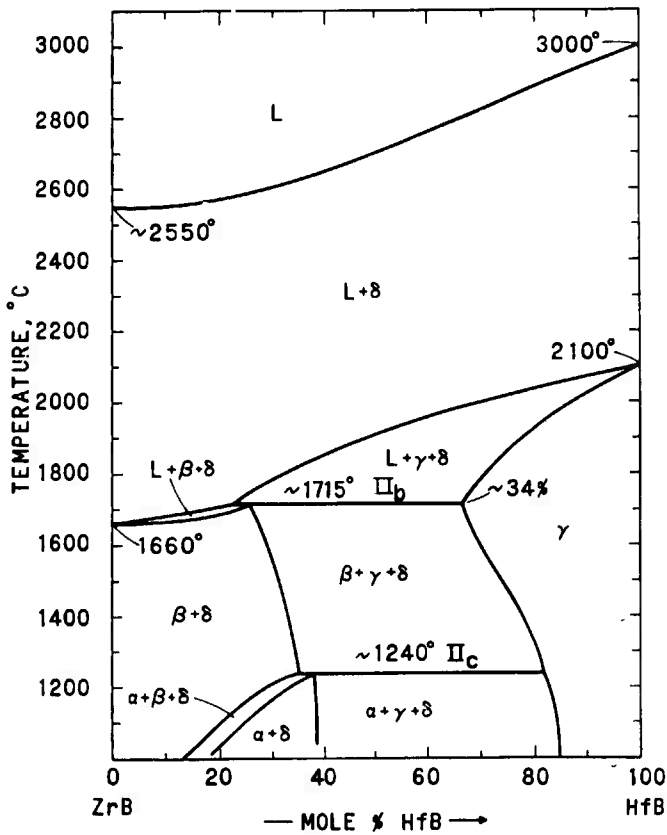

Figure 30. Isopleth Across 50 Atomic Percent Boron.

The compositional range of the monoboride phase in the ternary was therefore arrived at by evaluating alloys in this region of the system (≤ 35 atomic % boron). In view of the fact that the zirconium exchange in the monoboride solid solution was determined by

Figure 31. Zr-Hf-B (4/39/57): Arc-Melted Alloy Showing Large Diboride Grains (Light Grey) in a Non-Equilibrium Metal (Light)-Monoboride (Dark) Matrix. X150

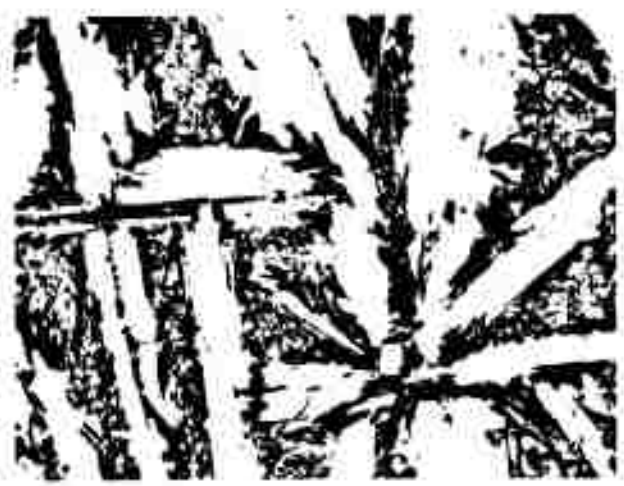

Figure 32. Zr-Hf-B (4/39/57): Arc-Melted (See Figure 31) and Equilibrated at 1400°C for 200 hrs. X150

Formation of Hafnium Monoboride Solid Solution (Dark) from the Diboride (Light Grey) and Metal (Light) After Prolonged Heat Treatment.

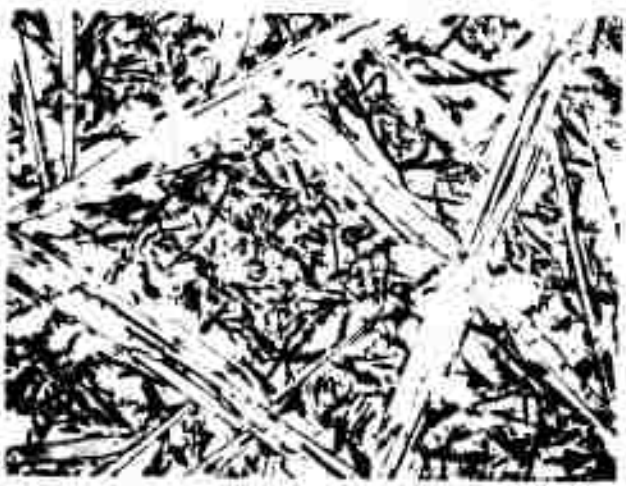

Figure 33. Zr-Hf-B (5/60/35): Arc-Melted Alloy Showing Non-Equilibrium Diboride Grains (Light Grey) in a Metal (Light) Monoboride (Dark) Matrix. X400

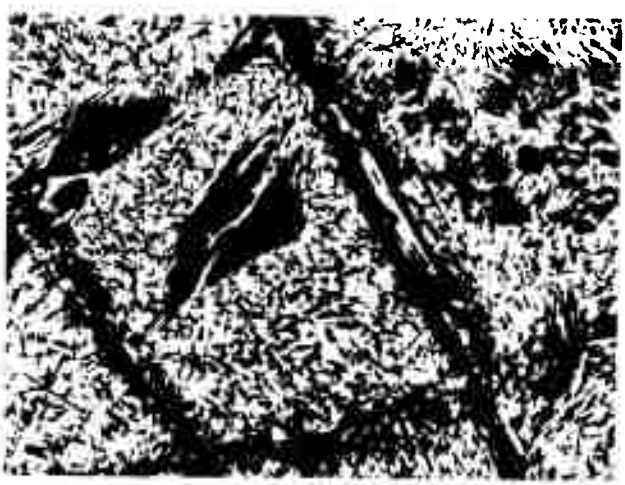

Figure 34. Zr-Hf-B (5/60/35): Arc-Melted (See Figure 33) and Equilibrated at 1400°C for 200 Hours. X225

Monoboride Phase (Long, Dark Grains) Formed from Diboride Grains in a Monoboride-Metal Matrix. Note that the Reaction has not Gone to Completion in One Grain.

these indirect means (X-ray and metallographic analysis of two and three-phased alloys), a rather large uncertainty should be associated with this value, i.e. $\pm$ 7 mole percent "zirconium monoboride" exchange.

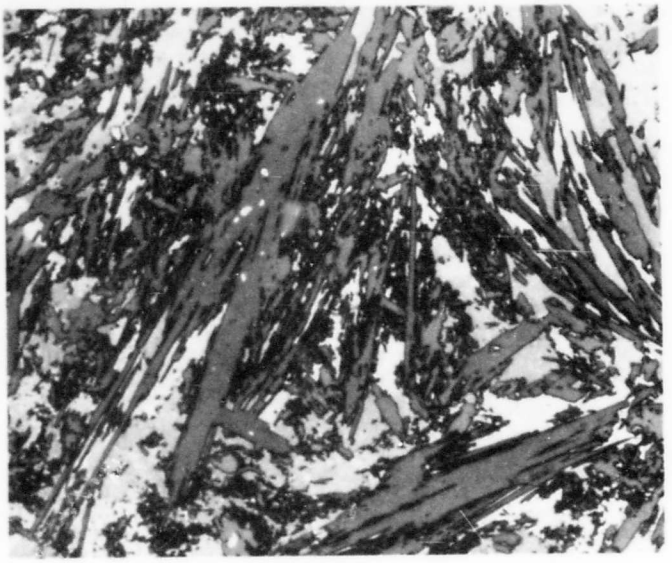

Figure 35. Zr-Hf-B (15/50/35): Rapidly Cooled from 1825°C. X675

Monoboride Solid Solution (Dark) in a Metal-Monoboride Matrix (Sample Did Not Exceed Peritectic Temperature).

Above 1715°C the three-phase regions, $L + \beta + \gamma$ and $L + \gamma + \delta$, progress towards the hafnium-boron binary system, and terminate in the binary eutectic (1880°C) and peritectic (2100°C) reactions respectively.

(2) Diboride Solid Solution

A total of eighteen melting point samples were used to investigate the maximum solidus of the diboride solution; the results are shown in Figure 36. Due to the fact that the diboride phase has such a limited range of homogeneity, maximum melting temperatures are

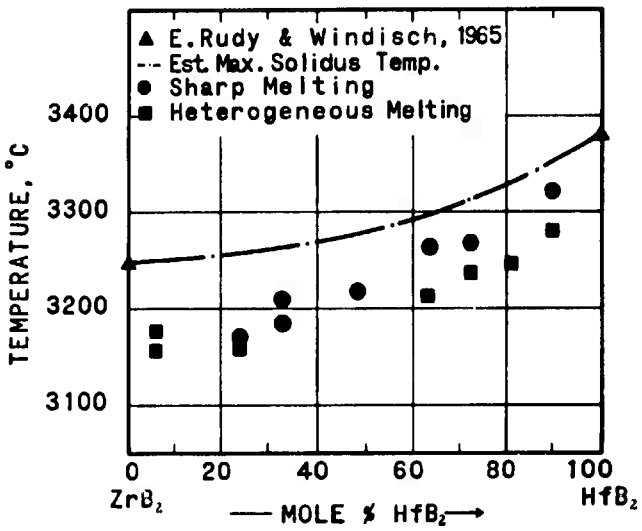

Figure 36. Experimentally Determined Melting Points of $(Zr,Hf)B_2$ Alloys and Estimated Maximum Solidus Temperatures.

very difficult to obtain. Rudy and Windisch[1,2] experienced this same difficulty while investigating the melting points of the binary diboride phases, and, since their work was much more exhaustive, the ternary melting curve was estimated using their end points in conjunction with present ternary melting point data. Metallographic and chemical analysis of the melting points showed that the majority of the alloys were to some extent two-phase (metal-diboride or boron-diboride, Figures 37 and 38); thus it can be assumed that the melting data obtained in the ternary investigations yielded temperatures somewhat below the actual maximum solidus curve. It can also be concluded from these results that the homogeneous limit of the diboride solid solution in the ternary system is very narrow.

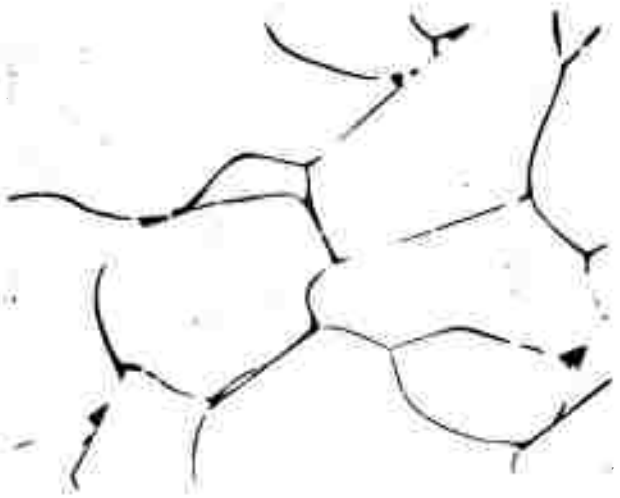

Figure 37. Zr-Hf-B (3/30/67): Sample Quenched from its Melting Point, 3280°C. X400

Diboride Grains in a Metal Matrix (Analyzed Boron Content: 65 Atomic Percent).

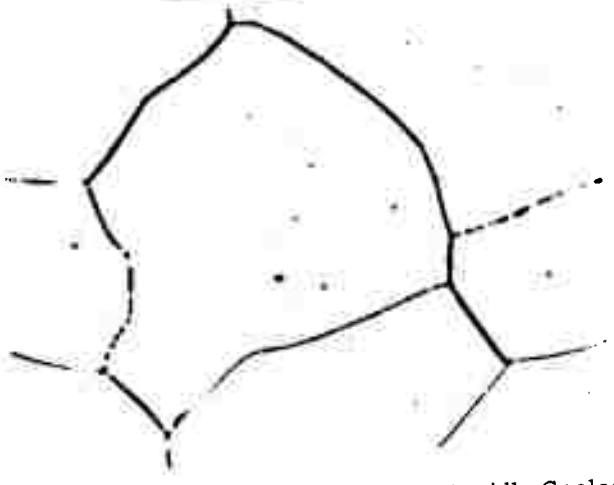

Figure 38. Zr-Hf-B (12/21/67): Sample Rapidly Cooled from its Melting Point, 3265°C. X1000

Nearly Single Phase Diboride with Boron at the Grain Boundaries (Analyzed Boron Content: 68 Atomic Percent).

Lattice parameter measurements of the melted alloys yielded results identical with those presented in Figure 24.

(3) Boron-Rich Phase Equilibria

This region of the ternary system received only a nominal amount of attention, since, because of the restricted temperature stability range of the ZrB_{12} phase as well as the small difference between the boron-rich eutectics of the binary systems, the phase equilibria would be very difficult to establish experimentally.

Metallographic investigation of arc-melted alloys indicated that the three-phase field ($\delta + \epsilon$ + B) extended quite far into the ternary; with an alloy at 90 atomic percent boron (Zr:Hf = 1:1), a considerable amount of the dodecaboride phase is observed (Figure 39).

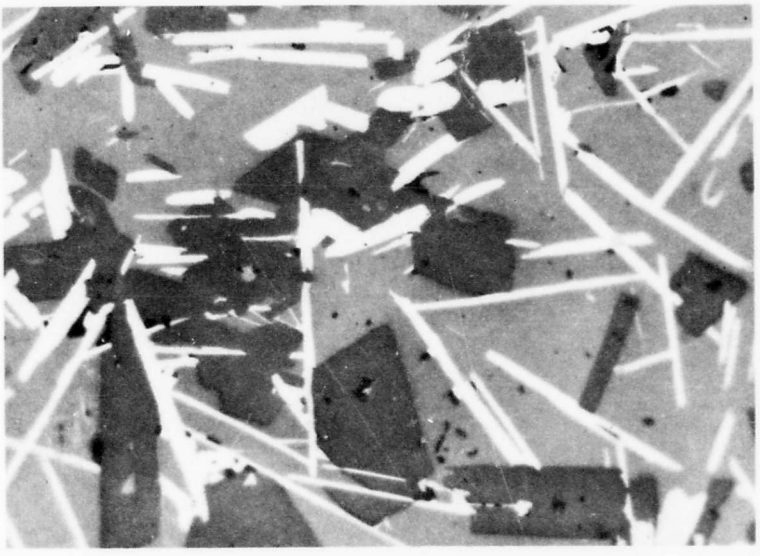

Figure 39. Zr-Hf-B (5/5/90): Arc-Melted Alloy Three-Phased: ZrB_{12} (Dark Grey) + $(Zr,Hf)B_2$ (Light) Boron (Grey). X650

Assuming that a ternary eutectic does not exist in this region, the two-over-two four-phase plane (Class II: $L + \delta \rightleftharpoons \epsilon + B$) that would result was estimated to occur at 2020 $\pm$ 20°C.

The aforementioned temperature sections are presented in Figures 40 and 49; in addition, the approximate liquidus projection for the ternary system is presented in Figure 50. The liquidus projection was estimated from the melting characteristics of the ternary alloys which were investigated.

As a further aid to understanding the temperature dependencies of various phase equilibria, isopleths across 30 and 50 atomic percent boron are given (Figures 4 and 30). For specific needs, additional isopleths can be developed by the reader with the use of the isothermal sections which are presented.

The system is summarized in an isometric drawing (Figure 2) covering the temperature range above 750°C in order to depict the overall phase relationships in the ternary zirconium-hafnium-boron system.

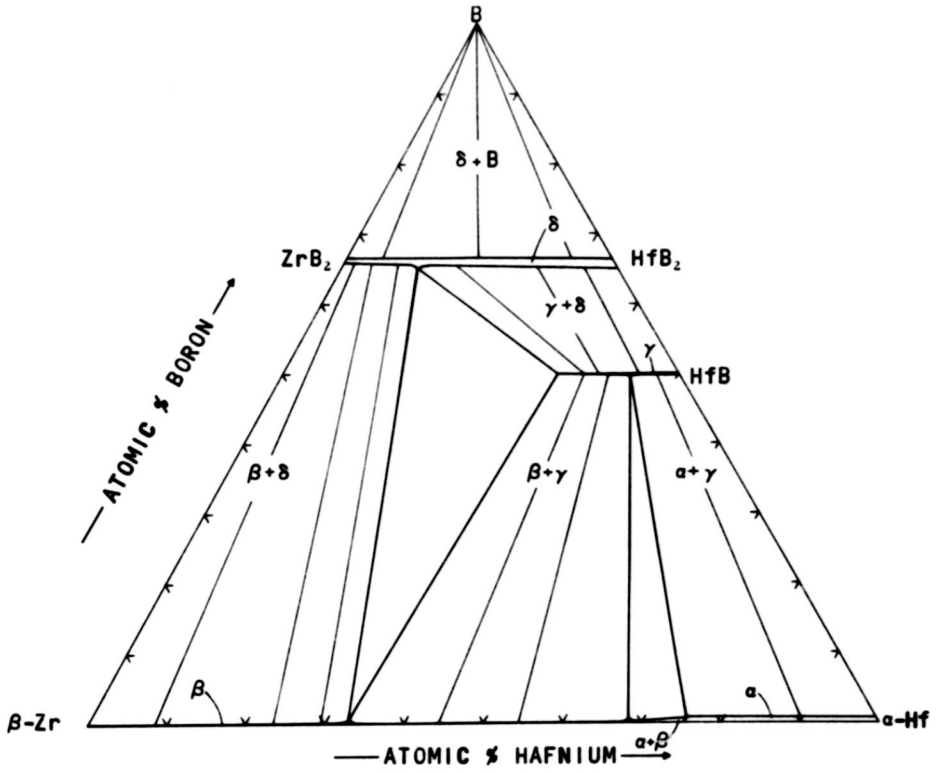

Figure 40. 1600°C Isotherm.

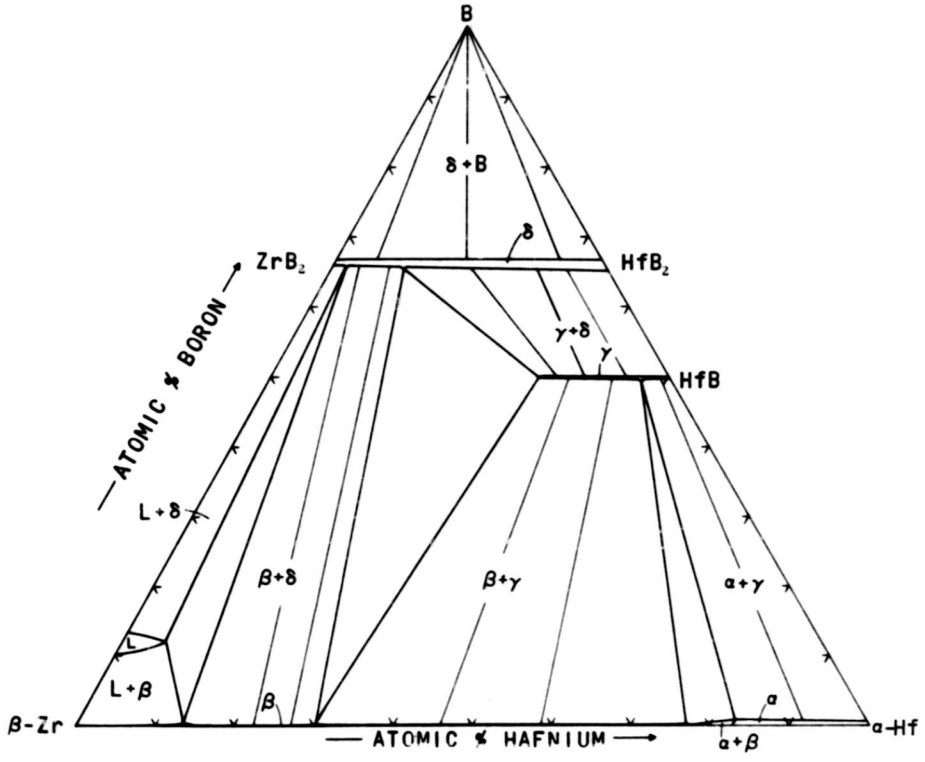

Figure 41. 1675°C Isotherm.

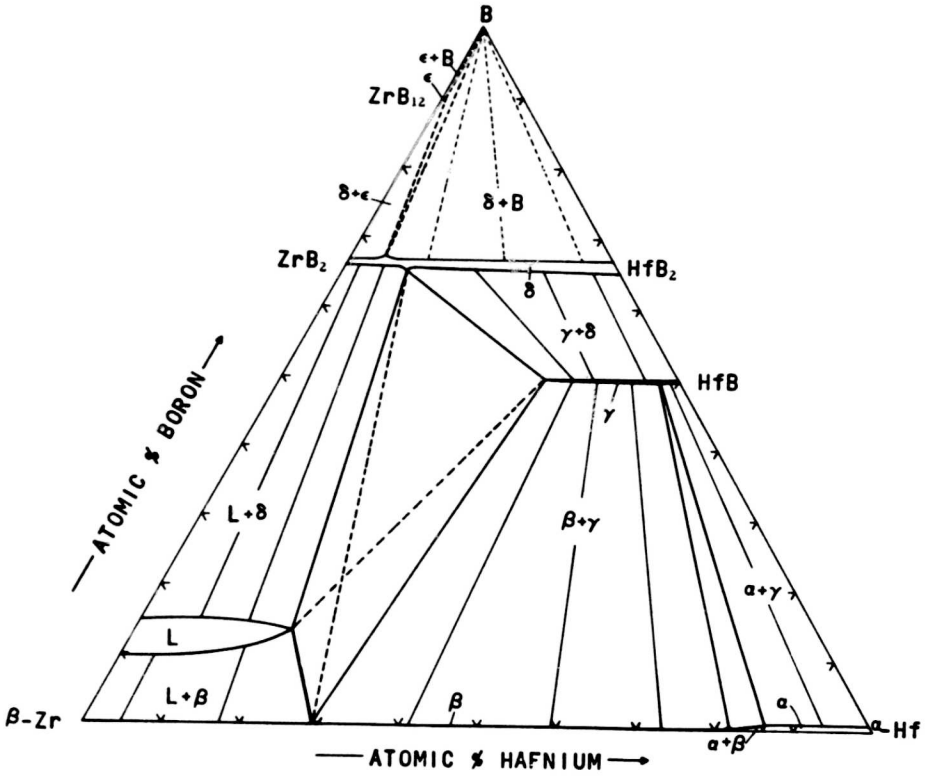

Figure 42. 1715°C Isotherm
[Four-Phase Reaction Plane ($L + \gamma \leftrightarrow \beta + \delta$)]

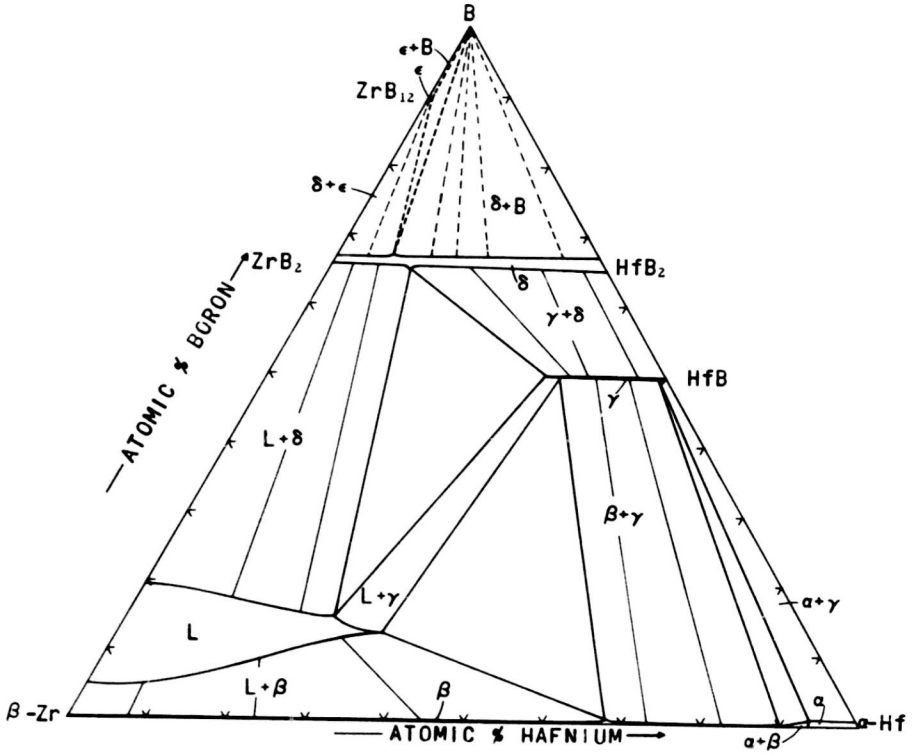

Figure 43. 1775°C Isotherm.

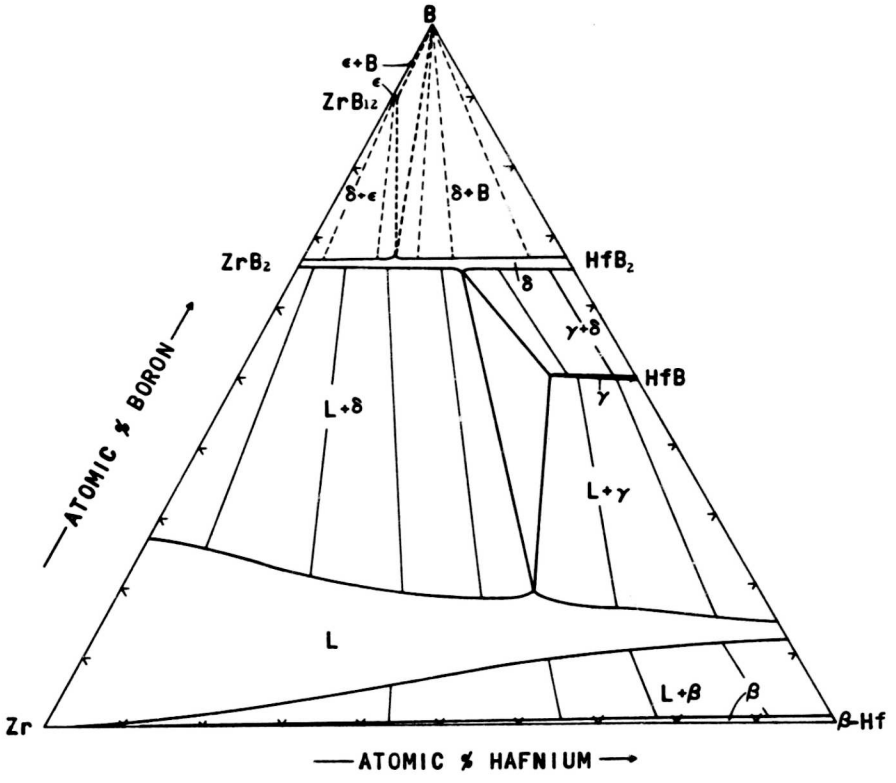

Figure 44. 1900°C Isotherm.

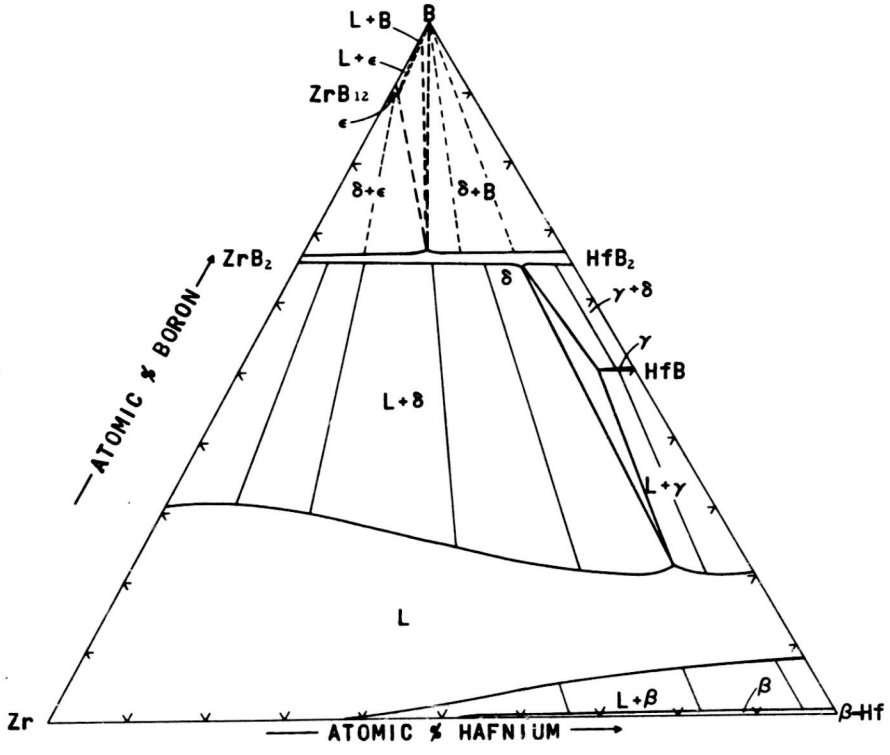

Figure 45. 2020°C Isotherm.
[Four-Phase Reaction Plane ($L + \delta \rightleftharpoons \epsilon + B$)]

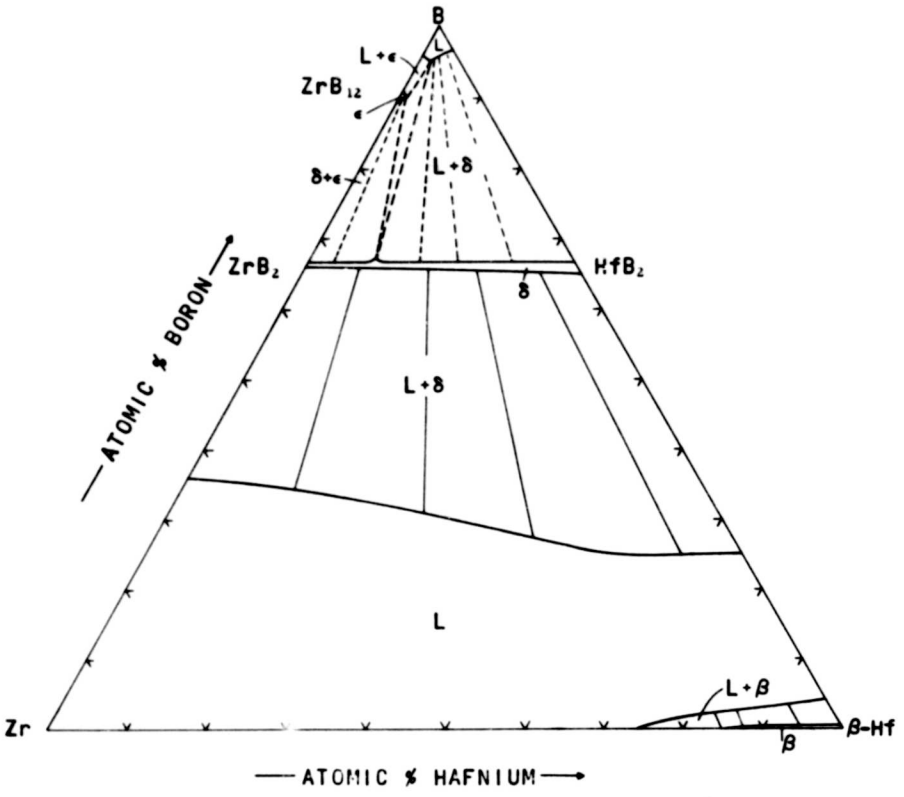

Figure 46. 2150°C Isotherm.

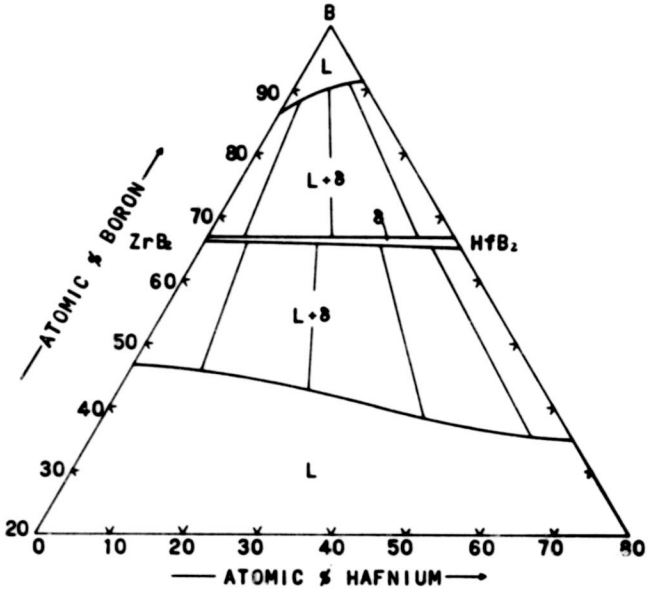

Figure 47. 2500°C Isotherm.

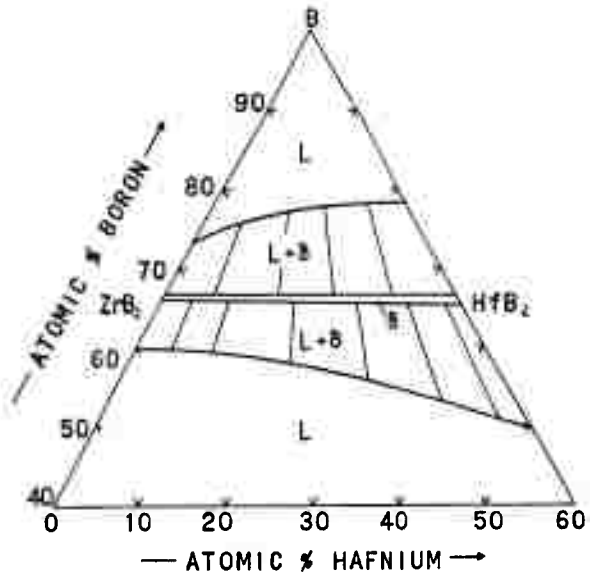

Figure 48. 3000°C Isotherm.

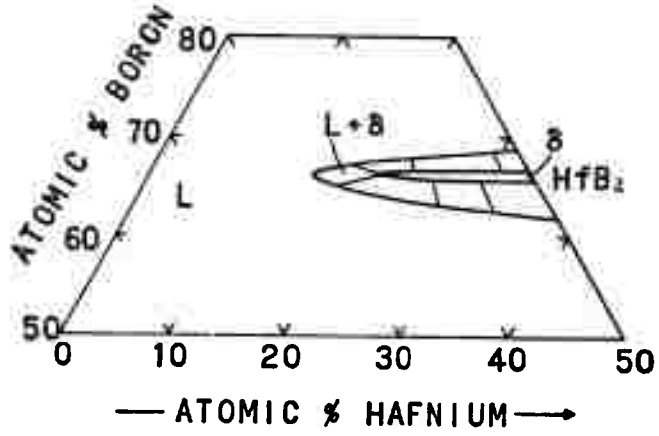

Figure 49. 3300°C Isotherm.

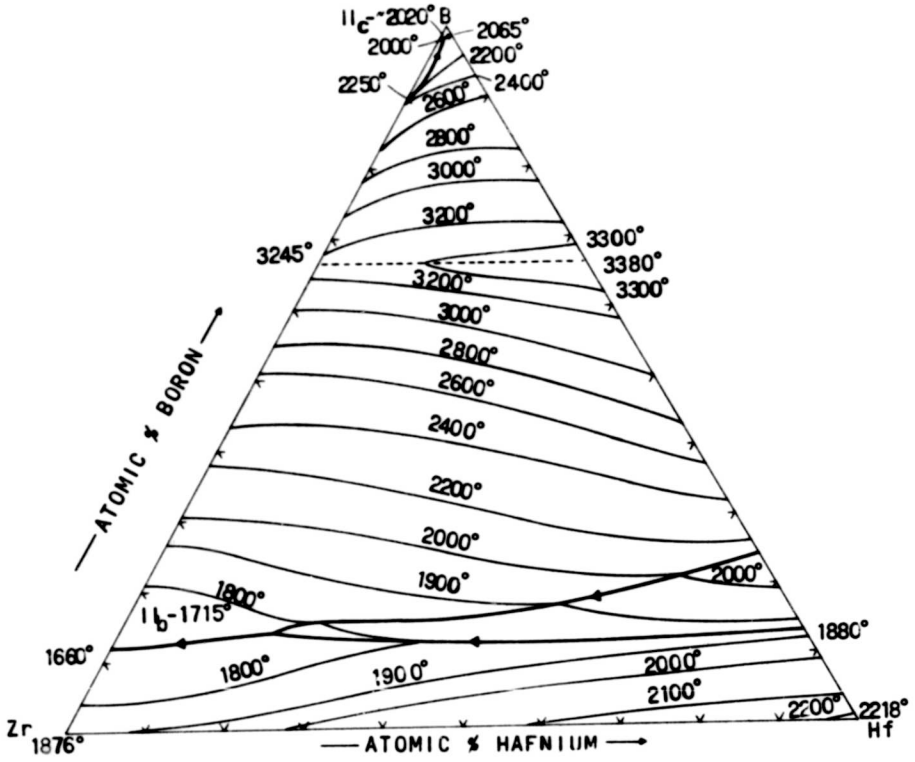

Figure 50. Liquidus Projection for the System Zirconium-Hafnium Boron.

---- Maximum $(Zr,Hf)B_2$ Solidus Temperature.

IV. DISCUSSION

A. THERMOCHEMICAL EVALUATION OF THE TERNARY EQUILIBRIA AT 1400°C

The free energy of formation (ΔG_f) for both the hafnium monoboride and the hypothetical "zirconium monoboride" phases have been estimated; in addition, the phase equilibria at 1400°C have been calculated using the experimentally established data as well as selected thermodynamic values for the binary phases. The computations were carried out using the thermochemical approach for multi-phase equilibria derived by E. Rudy[37].

Using Rudy's method[37] to extract the thermodynamic data from the ternary system at hand, the assumptions were made that the solid solutions behave ideally and that line-compounds are formed. From the experimentally established lattice parameters for the metal and diboride solutions, as well as the α-β transformation curves for the metal solutions it can be concluded that these solutions behave nearly ideally, and it would be unlikely that the monoboride solid solution would behave otherwise. Since each solid solution exhibits a boundary which has a nearly constant boron concentration, the line-compound requirement is also fulfilled.

From the experimentally established phase relationships at 1400°C (Figure 23), the decomposition energy of the hafnium monoboride phase can be calculated. At this temperature the HfB solid solution disproportionates into the β-metal and diboride solid solutions, thus one obtains for the reaction:

$$HfB_{<ss>} \longrightarrow 0.5\ Hf_{<ss>} + 0.5\ HfB_{2\ <ss>} \qquad (1)$$

$$-\Delta G_{Z_{HfB}} = 0.5\ \Delta\bar{G}_{HfB_2} + 0.5\ \Delta\bar{G}_{\beta\text{-}Hf} - \Delta\bar{G}_{HfB} \qquad (\ )$$

where

$\Delta G_{Z_{HfB}}$ = free energy of disproportionation of the HfB phase

$\Delta\bar{G}_{HfB_2} = RT \ln X_{HfB_2}$ = relative partial molar free energy of the HfB_2 in the diboride solid solutions. (similarly for the $\Delta\bar{G}_{Hf}$ and $\Delta\bar{G}_{HfB}$)

X_{HfB_2} = mole fraction of HfB_2 in the diboride solid solution (similarly for X^{β}_{Hf}, X_{HfB}).

From this relationship the value calculated for the free energy of disproportionation of the hafnium monoboride phase was 2620 $\pm$ 400 cal/mole;

similarly a ΔG_Z value for the hypothetical "ZrB" phase was determined to be -3450 $\pm$ 600 cal/mole. The uncertainties assigned to the values are primarily a result of the fact that the extent of the zirconium exchange in the hafnium monoboride phase is not known exactly.

With the ΔG_Z values for the monoboride phases in conjunction with the free energies of formation of respective binary diborides, the free energies of formation for HfB and "ZrB" can be determined. L. Kaufman[38] has recently evaluated the ΔG values for various diboride phases; values of $\Delta G_{ZrB_2} \approx \Delta G_{HfB_2} \approx$ -63,200 cal/mole were interpolated for 1400°C from this data. Using the relationship

$$\Delta G_{HfB} = 0.5\,\Delta G_{HfB_2} - \Delta G_{Z_{HfB}} + 0.5\,\Delta G_{Hf}^{\alpha \rightarrow \beta} \qquad (3)$$

where $\Delta G_{Hf}^{\alpha \rightarrow \beta}$ is the free energy of transformation of hafnium from the α- to β- state, a value of ΔG_{HfB} = -34,100 $\pm$ 1000 cal/mole was determined. In an identical fashion the free energy of formation for the "zirconium monoboride" phase was derived, i.e., $\Delta G_{ZrB} \approx$ -28,200 $\pm$ 1500 cal/mole.

Using the above data, an attempt was made to calculate the phase equilibria at 1400°C. Since four phases ($\alpha_{<ss>}$, $\beta_{<ss>}$, $\gamma_{<ss>}$, and $\delta_{<ss>}$) are present in the metal rich portion of the ternary system, and due to the fact that the zirconium monoboride does not exist, two three-phase fields must be present in this portion of the ternary system. In order to establish the correct three-phase equilibria at this temperature, the following conditional equations must be fulfilled:

$$\left(\frac{\partial \Delta G_1}{\partial X_u}\right)_{T,P} = \left(\frac{\partial \Delta G_2}{\partial X_v}\right)_{T,P} = \left(\frac{\partial \Delta G_3}{\partial X_w}\right)_{T,P} \qquad (4)$$

and

$$(v-w)\ \Delta\bar{G}_u + (w-u)\ \Delta\bar{G}_v + (u-v)\ \Delta\bar{G}_w = 0 \qquad (5)$$

where

ΔG = Gibbs free energies of the respective phases

$\Delta\bar{G}$ = relative partial molar free energy of the respective phases

X = mole fraction of the corresponding phase in the respective solid solution

u, v, and w = boron content of the solid solution expressed as mole ratio of boron to metal

P = pressure (atmospheres)

T = absolute temperature (°K)

Evaluation of these conditions is best done graphically. The free energy gradient curves for the α-, β-, γ-, and δ-solid solutions can be constructed knowing

$$\frac{\partial \Delta G_{(Zr,Hf)B_i}}{\partial X_{(Zr,Hf)B_i}} = \Delta G_{HfB_i} - \Delta G_{ZrB_i} + RT \ln \frac{X_{HfB_i}}{1-X_{HfB_i}} \qquad (6)$$

where R is the gas constant. For the α-β metal solid solutions the two terms on the right in equation (6) are equal to the free energy of transformation from $\alpha \rightarrow \beta$, $(\Delta G^{\alpha \rightarrow \beta})$, and can be expressed as,

$$\Delta G_{Zr}^{\alpha \rightarrow \beta} = 1040 \left(1 - \frac{T}{1145}\right) \qquad (7)$$

$$\Delta G_{Hf}^{\alpha \rightarrow \beta} = 1870 \left(1 - \frac{T}{2083}\right) \qquad (8)$$

With the above equations and using the proper thermodynamic as well as experimental data, the free energy gradient curves for the four solid-solutions were constructed and are given in Figure 51.

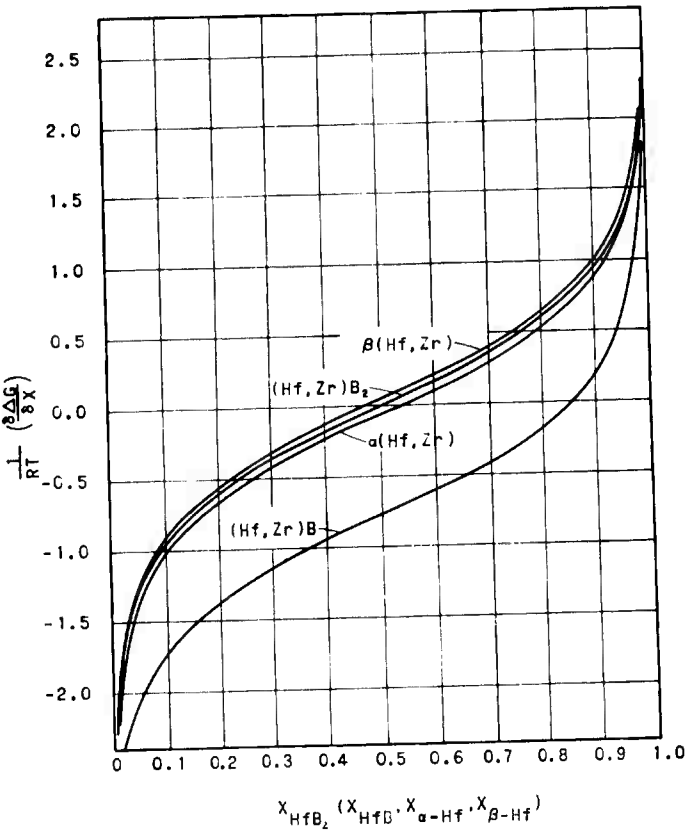

Figure 51. Free Energy Gradient Curves for the α-, β-, γ-, and δ-Solid Solutions at 1400°C.

To determine the three-phase equilibria, two additional pieces of information are needed; these are the location of the phase boundaries of the α- and β-phases in the metal binary system and the location of the terminal concentration of the monoboride solid solution into the ternary system.

The location of the α-β-phase boundaries can be established by simultaneously solving the equations below[39] for the mole fraction of either zirconium or hafnium in the α- and β-phases.

$$RT \ln \frac{X^{\alpha}_{Zr}}{X^{\beta}_{Zr}} = \Delta H^{\alpha \rightarrow \beta}_{Zr} \left(1 - \frac{T}{T_{\alpha \rightarrow \beta Zr}}\right) \quad (9)$$

and

$$RT \ln \frac{X^{\alpha}_{Hf}}{X^{\beta}_{Hf}} = \Delta H^{\alpha \rightarrow \beta}_{Hf} \left(1 - \frac{T}{T_{\alpha \rightarrow \beta Hf}}\right) \quad (10)$$

where

$X^{\alpha}_{Zr(Hf)}$ = mole fraction of zirconium (hafnium) in the α-solid solution

$X^{\beta}_{Zr(Hf)}$ = mole fraction of zirconium (hafnium) in the β-solid solution

$\Delta H^{\alpha \rightarrow \beta}_{Zr(Hf)}$ = enthalpy of transformation from the α to the β form for zirconium (hafnium)

$T_{\alpha \rightarrow \beta Zr(Hf)}$ = α-β transformation temperatures (°K) of zirconium (hafnium)

At 1400°C the α-solid solution extended to 53 atomic percent hafnium and the β-solid solution to 58.5 atomic percent hafnium.

The location of the terminal composition of the monoboride solid solution is obtained graphically by plotting $\Delta G_{Z_{HfB}}$ as a function of X_{Hf} (equation 2); the intersection of the experimentally determined free energy of disproportion with the resulting curve yields the mole fraction of hafnium monoboride in the solid solution. The value was determined to be 80 mole percent HfB.

The 1400°C section can now be assembled using the above calculated vertices for the three-phase regions, in conjunction with the gradient curves; the selection of the proper three-phase equilibria is intuitively obvious once the conditional points are plotted on the gradient curves (Figure 52).

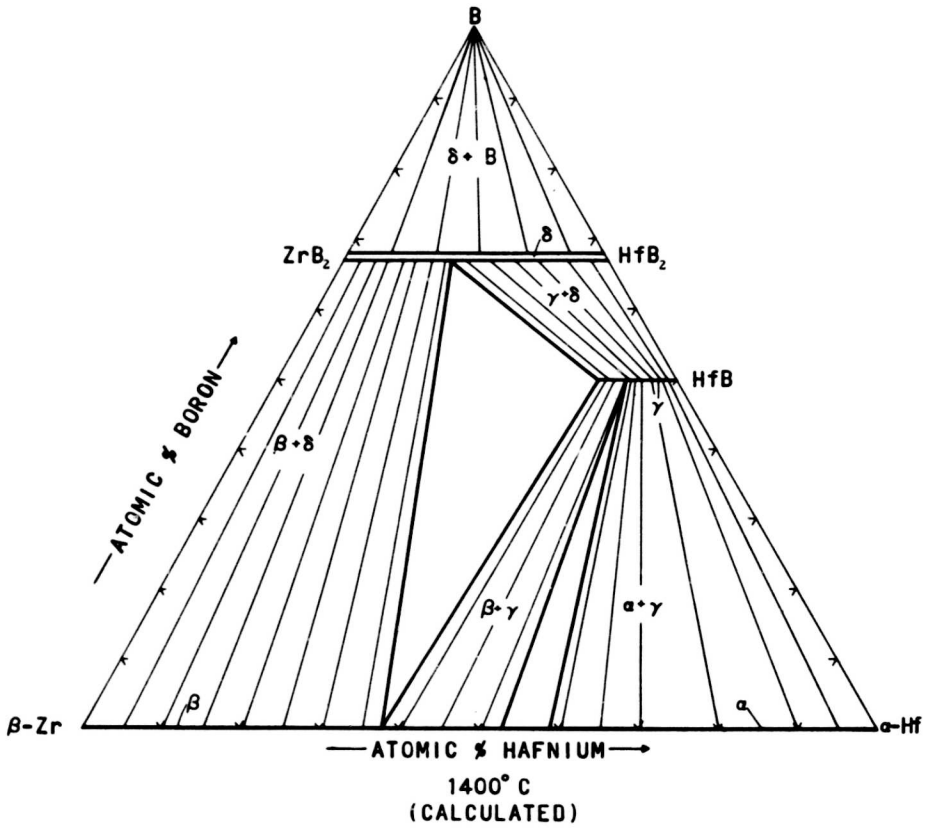

Figure 52. Calculated 1400°C Isothermal Section.

The tie-line distribution in the five two-phase regions ($\beta + \delta$, $\beta + \gamma$, $\alpha + \beta$, $\alpha + \gamma$, $\gamma + \delta$) can readily be established from the gradient curves. For the sake of completeness, the tie-lines in the $\delta + \beta$ region are also drawn; although no calculations were performed,it is apparent that all diboride compositions are in equilibrium with the boron phase.

A comparison of the experimental and theoretical section at 1400°C (Figures 23 and 52) show that they are in good agreement with each other. The difference in the tie-line distribution in the monoboride-diboride two-phase region ($\gamma + \delta$) is most likely due to the fact that samples in this

region obtained equilibrium extremely slow, and, therefore, it is felt that the calculated section more correctly represents the tie-lines distribution between these two-phases. It should also be noted that the experimentally established data indicated that the zirconium diboride to be slightly more stable than the hafnium diboride at 1400°C, whereas the literature[38] shows the two to be equally stable.

B. APPLICATIONS

Of the borides of the group IVa, Va, and VIa refractory metals, the diborides of zirconium and hafnium show the most promise for high temperature application. Not only are they the most refractory, but they also exhibit superior oxidation characteristics; it has been reported that hafnium diboride displays the best oxidation resistance of the borides of this group[27]. However, because of their extreme brittleness and susceptibility to failure by thermal shock, single phase diboride materials cannot be used for most applications. Composite systems are therefore necessary to overcome these inherent deficiencies; however, materials compatibility (chemical as well as physical) poses a formidable problem for the selection of promising systems. Here, established phase equilibrium relationships greatly enhance the proper selection of systems which are to be developed.

From the investigation of the zirconium-hafnium-boron system, reinforcement of the zirconium-rich diboride solid solution with the zirconium-rich metal phase appears to be promising. Hafnium additions to zirconium diboride-metal composites not only will increase the melting temperatures of these systems but also will most probably improve the oxidation characteristics. It should be mentioned that recent investigations have shown that the metal-rich diboride composites ($Zr+ZrB_2$ and $Hf + HfB_2$) exhibit better oxidation resistance than single-phase structures[27].

With hafnium-rich composites the intermediate monoboride phase is formed, therefore, this region of this system appears to be less desirable for many applications. However, the extremely slow rate of formation of this phase might allow the non-equilibrium metal-diboride composites to be used for short time applications (see Figure 37; two-phase alloy, metal + diboride).

REFERENCES

1. E. Rudy and St. Windisch: AFML-TR-65-2, Part I, Vol. VIII, October 1965.

2. E. Rudy and St. Windisch: AFML-TR-65-2, Part I, Vol. IX, October 1965.

3. E. T. Hayes and D. K. Deardorff: Work quoted in "The Metallurgy of Hafnium", Ed. D. E. Thomas and E. T. Hayes.

4. F.N. Rhines: "Phase Diagrams in Metallurgy", McGraw-Hill (1956).

5. J. D. Fast: J. Appl. Phys., 23 (1952) 350-351.

6. D. K. Deardorff and H. Kato: USBM-4-426 (1958).

7. A. Taylor and N. J. Doyle: WADD-TR-60-132 (1960); also J. Less Common Metals, 3 (1961) 265.

8. N. J. Grant and B. C. Giessen: WADD-TR-60-132 (1960).

9. R. G. Ross and W. Hume-Rothery: J. Less Common Metals, 5 (1963) 258.

10. R. G. Bedford: J. Appl. Physics, 36 (1965) 113.

11. P.A. Romans, O.G. Pasche, and H. Kato: J. Less Common Metals, 8 (1965) 213.

12. E. Rudy: AFML-TR-65-2, Part I, Vol. IV, Sept. 1965.

13. P. Duwez: Trans. AIME, 191 (1951) 765.

14. E. Rudy, D. P. Harmon, and C. E. Brukl: AFML-TR-65-2, Part I, Vol. II, May 1965.

15. C. E. Ells and A.D. McQuillan: J. of Inst.of Metals, 85 (1956), 89-96.

16. M. Hansen: "Constitution of Binary Alloys", McGraw-Hill, New York (1958).

17. B. Post and W. Glaser: J. Chem. Phys., 20 (1952) 1050.

18. F. W. Glaser: Trans. AIME 144 (1952) 391.

19. F. W. Glaser and B. Post: Trans. AIME, 197 (1953) 1117.

20. R. Kiessling; Acta. Chem. Scand., 3 (1949) 90.

21. L. Brewer, D.L. Sawyer, D.H. Templeton, and C. H. Dauben: J. Amer. Ceram. Soc., 34 (1951), 173.

References (continued)

22. E. Rudy and F. Benesovsky: Mh. Chem., 92 (1961) 415.

23. W. Schedler: Thesis, Technische Hochschule Graz, Austria (1951).

24. C. Agte: Thesis, Technische Hochschule, Berlin, 1931.

25. K. Moers: Z. anorg. allg. Chemie, 198 (1931), 262.

26. F.W. Glaser, D. Moskowitz and B. Post: J. of Metals (Sept 1953) 1114.

27. L.Kaufman, and E.V. Clougherty: RTD-TDR-63-4096, Part II (Feb-1965).

28. R. Kieffer, F. Benesovsky, and E.R. Honak: Z. anorg. allg. Chemie, 268 (1952), 191.

29. B. Post, F. W. Glaser, and D. Moskowitz: Acta Met, 2 (1954), 20.

30. K. C. Antony and W. V. Cummings: GEAP 3530 (1960).

31. R. Kieffer and F. Benesovsky: "Hartstoffe" Springer, Vienna, (1963).

32. A. Taylor and B.J. Kagle: "Crystallographic Data on Metal and Alloy Structures", Dover Publications, New York (1963).

33. H.D. Heetderks, E. Rudy, and T. Eckert: Planseeber, f. Pulvermetallurgie, 13 (1965) 105-125.

34. E. Rudy, St. Windisch, and Y.A. Chang: AFML-TR-65-2, Part I, Vol. I. (Jan. 1965).

35. E. Rudy and St. Windisch: AFML-TR-65-2, Part I, Vol. VII (Oct 1965).

36. R. B. Russell, J. Appl. Phys., 24 (1953) 232.

37. E. Rudy: Z. Metallkde., 54 (1963) Parts I and II, 112-122 and 213-223.

38. L. Kaufman: In- "Compounds of Interest in Nuclear Reactor Technology" J.T. Waber, P. Chiotti, and W.N. Miner, Ed.IMD Special Report No. 13 (AIME) 1964.

39. R.A. Swalin: "Thermodynamics of Solids", Wiley, New York (1962).

DOCUMENT CONTROL DATA - R&D

(Security classification of title, body of abstract and indexing annotation must be entered when the overall report is classified)

1 ORIGINATING ACTIVITY *(Corporate author)* Materials Research Laboratory Aerojet-General Corporation Sacramento, California	2a REPORT SECURITY CLASSIFICATION Unclassified 2b GROUP N.A.

3 REPORT TITLE

Ternary Phase Equilibria in Transition Metal-Boron Carbon-Silicon Systems

Part II. Ternary Systems, Volume VI. Zr-Hf-B System

4 DESCRIPTIVE NOTES *(Type of report and inclusive dates)*

Documentary Report

5 AUTHOR(S) *(Last name, first name, initial)*

Harmon, David P.

6 REPORT DATE	7a TOTAL NO. OF PAGES	7b NO. OF REFS
November, 1965	64	39

8a CONTRACT OR GRANT NO.	9a ORIGINATOR'S REPORT NUMBER(S)
AF 33(615)-1249	AFML-TR-65-2 Part II, Vol. VI.
b PROJECT NO. 7350	
c Task No. 735001	9b OTHER REPORT NO(S) *(Any other numbers that may be assigned this report)*
d	N.A.

10 AVAILABILITY/LIMITATION NOTICES

This document is subject to special export controls and each transmittal to foreign governments or foreign nationals may be made only with prior approval of Metals & Ceramics Div., AF Materials Laboratory, Wright-Patterson AFB, Ohio.

11 SUPPLEMENTARY NOTES	12 SPONSORING MILITARY ACTIVITY
	AFML(MAMC) Wright-Patterson AFB, Ohio, 45433

13 ABSTRACT

The ternary system zirconium-hafnium-boron has been established for temperatures above 750°C with the aid of melting point, X-ray, and metallographic investigations of chemically analyzed alloys.

A brief thermochemical evaluation of the system was made at 1400°C, and the Gibbs free energies of formation for both the hafnium monoboride and hypothetical "zirconium monoboride" were calculated.

The zirconium-hafnium system was reviewed using differential-thermal analytical techniques, and the proposed binary diagram is given.

DD FORM 1 JAN 64 1473

Unclassified

Security Classification

Unclassified
Security Classification

14. KEY WORDS	LINK A		LINK B		LINK C	
	ROLE	WT	ROLE	WT	ROLE	WT
Borides Phase Equilibria Ternary System Zirconium-Hafnium Boron						

INSTRUCTIONS

1. ORIGINATING ACTIVITY: Enter the name and address of the contractor, subcontractor, grantee, Department of Defense activity or other organization *(corporate author)* issuing the report.

2a. REPORT SECURITY CLASSIFICATION: Enter the overall security classification of the report. Indicate whether "Restricted Data" is included. Marking is to be in accordance with appropriate security regulations.

2b. GROUP: Automatic downgrading is specified in DoD Directive 5200.10 and Armed Forces Industrial Manual. Enter the group number. Also, when applicable, show that optional markings have been used for Group 3 and Group 4 as authorized.

3. REPORT TITLE: Enter the complete report title in all capital letters. Titles in all cases should be unclassified. If a meaningful title cannot be selected without classification, show title classification in all capitals in parenthesis immediately following the title.

4. DESCRIPTIVE NOTES: If appropriate, enter the type of report, e.g., interim, progress, summary, annual, or final. Give the inclusive dates when a specific reporting period is covered.

5. AUTHOR(S): Enter the name(s) of author(s) as shown on or in the report. Enter last name, first name, middle initial. If military, show rank and branch of service. The name of the principal author is an absolute minimum requirement.

6. REPORT DATE: Enter the date of the report as day, month, year; or month, year. If more than one date appears on the report, use date of publication.

7a. TOTAL NUMBER OF PAGES: The total page count should follow normal pagination procedures, i.e., enter the number of pages containing information.

7b. NUMBER OF REFERENCES: Enter the total number of references cited in the report.

8a. CONTRACT OR GRANT NUMBER: If appropriate, enter the applicable number of the contract or grant under which the report was written.

8b, 8c, & 8d. PROJECT NUMBER: Enter the appropriate military department identification, such as project number, subproject number, system numbers, task number, etc.

9a. ORIGINATOR'S REPORT NUMBER(S): Enter the official report number by which the document will be identified and controlled by the originating activity. This number must be unique to this report.

9b. OTHER REPORT NUMBER(S): If the report has been assigned any other report numbers *(either by the originator or by the sponsor)*, also enter this number(s).

10. AVAILABILITY/LIMITATION NOTICES: Enter any limitations on further dissemination of the report, other than those imposed by security classification, using standard statements such as:

(1) "Qualified requesters may obtain copies of this report from DDC."

(2) "Foreign announcement and dissemination of this report by DDC is not authorized."

(3) "U. S. Government agencies may obtain copies of this report directly from DDC. Other qualified DDC users shall request through _____."

(4) "U. S. military agencies may obtain copies of this report directly from DDC. Other qualified users shall request through _____."

(5) "All distribution of this report is controlled. Qualified DDC users shall request through _____."

If the report has been furnished to the Office of Technical Services, Department of Commerce, for sale to the public, indicate this fact and enter the price, if known.

11. SUPPLEMENTARY NOTES: Use for additional explanatory notes.

12. SPONSORING MILITARY ACTIVITY: Enter the name of the departmental project office or laboratory sponsoring *(paying for)* the research and development. Include address.

13. ABSTRACT: Enter an abstract giving a brief and factual summary of the document indicative of the report, even though it may also appear elsewhere in the body of the technical report. If additional space is required, a continuation sheet shall be attached.

It is highly desirable that the abstract of classified reports be unclassified. Each paragraph of the abstract shall end with an indication of the military security classification of the information in the paragraph, represented as *(TS), (S), (C), or (U)*.

There is no limitation on the length of the abstract. However, the suggested length is from 150 to 225 words.

14. KEY WORDS: Key words are technically meaningful terms or short phrases that characterize a report and may be used as index entries for cataloging the report. Key words must be selected so that no security classification is required. Identifiers, such as equipment model designation, trade name, military project code name, geographic location, may be used as key words but will be followed by an indication of technical context. The assignment of links, rules, and weights is optional.

Unclassified
Security Classification